Thesis N°:

Ministry of Higher Education and Scientific Research

University of Oran 2 Mohamed Ben Ahmed

Faculty of Earth and Universe Sciences

Department of Geology

Thesis for the obtention of the academic Master Diploma in earth science

Option: Geology of sedimentary basins (GBS).

Theme:

Paleoenvironments and taphonomy of shell concentrations from the Upper Jurassic of the Saharan Atlas, Algeria.

Presented by: Mr. BENMOUSSA Mahmoud Abderahmenne.

Board of examiners:

President: Mr. BENDELLA Mohamed (Professor)

Supervisor: Mr. SADJI Radouane (associate professor B)

Examiner: Mr. BOUALEM Noureddine (associate professor A)

Academic year: **2024/2025**

In the memory of my mother

I hope you are proud

...

ACKNOWLDGMENT

I would like to begin by expressing my deepest gratitude to my supervisor, **Mr. SADJI Radouane** (Maître de conferences B at university of Oran 2), for his constant guidance, support, and trust throughout the development of this thesis. His expertise, patience, and high standards have been both a challenge and a source of motivation. I am sincerely thankful for the time, knowledge, and encouragement he has generously provided at every stage of my research.

My special thanks go to the president of the jury**, Mr. BENDELLA Mohamed** (Professor at university of Oran 2), for accepting to chair my thesis defense and for their interest in my work. But most importantly I want to express my gratitude for his encouragement and teachings since day one, and made me look at things in a different way.

I warmly thank **Mr. BOUALEM Noureddine** (Maître de conferences A at university of Oran 2), for accepting to attend as an examiner and their valuable time, without forgetting his teaching during the previous years.

Many thanks to **Mr. FÜRSICH T. Franz** (Professor at *GeoZentrum* Nordbayern, Elangen Germany), for the identification of the oysters, we thank also **RADULOVIĆ Barbara V.** (University of Belgrade, Belgrade, Serbia) for the identification of the Brachiopods.

It is with great appreciation that I thank all the teachers that contributed to my formation throughout my academic journey including **MR. OUALI MEHADJI Aek, Mr. BOUAMEUR Mansor, Mr. BELKHDIM Salim, Mr. MAHBOUBI Younes.**

Finally, I extend my heartfelt thanks to my dear friends, **Anes, Boujlal, Djaouad, Faycal, Imed, Karim, Mahdi, Yassine, Youcef, Younes**, whose support, motivation, and friendship helped me stay balanced and focused throughout this journey. Your presence made the difficult days easier and the good days more meaningful.

Thank you so much everyone!

BENMOUSSA Mahmoud abderahmenne

DEDICATION

*First and foremost, I thank **God**, the Most Merciful, for granting me the strength, clarity, and perseverance to carry this work to completion.*

*I dedicate this thesis with deep love and eternal gratitude to the memory of **my dear mother** hoping I fulfilled her wish. Though she is no longer with me, her love, sacrifices, and values continue to shape who I am. Her memory remains a constant source of strength and motivation in my life.*

*To **my father**, whose support and patience have been unwavering thank you for believing in me even when things were difficult. Your presence mean more than words can express. To **my sister**, thank you for your kindness, your understanding, and for being by my side through every step of this journey.*

*I also express my sincere gratitude to **my teachers**, who have guided me with their knowledge and dedication. Their efforts have not only shaped this research but also helped me grow as a person and as a geologist.*

*Finally, to **my team** thank you for your, unconditional friendship, collaboration, your insights, and your shared commitment to excellence. Working with you has been one of the most rewarding parts of this experience.*

"We are made of all those who built us, guided us, and stood by us"

ABSTRACT

The Sfissifa Formation, of Upper Jurassic age, crops out in the Djebel Amour and is well exposed at Djebel Er Roken, southwest of the Sfissifa village, approximately 45 km east of the El Bayadh city. This study explores the paleoenvironmental, and taphonomic features of the shell beds that characterize this formation, aiming to decipher their genesis and depositional settings.

The lithological features of the Sfissifa Formation include interbedded marls, gypsum-rich layers, sandstones, dolostones, oolitic limestones, and its distinctive carbonate-dominated shell beds. These shell beds display various sedimentary structures such as trough cross-bedding and erosive bases, represent one of the most characteristic facies of this formation. Two brachiopod-rich marl levels have been identified and used as key biostratigraphic markers, allowing the formation to be dated to the late Kimmeridgian (*Xestosina arguta*, marking the transition from the *Eudoxus* Zone to the base of the *Autissiodorensis* Zone) and early Tithonian (*Xestosina sera*, representing the *Gigas* Zone, *Gravesiana* Subzone).

Microfacies analysis revealed a diversity of carbonate textures including rudstones, packstones, grainstones, and floatstones dominated by shell remains, ooids, bivalves, associated with quartz grains. These variations, along with associated sedimentary structures, indicate deposition in a range of shallow-marine environments, from storm-dominated shoals and inner ramp settings to more stable lagoonal and restricted marine conditions. Features such as hummocky cross-stratification, bioturbation, and evaporitic layers reflect complex fluctuations in energy conditions and water chemistry throughout the studied time span.

The shell beds show clear signs of reworking, and selective preservation, all pointing to episodic high-energy episodes that shaped their accumulation. Taphonomic evidences including shell fragmentation, articulation, and orientation in addition of the microfacies data underscores a strong relationship between physical depositional processes, and the nature of shell concentration.

Key-words: Shell-beds, Sfissifa, El-Bayadh, upper-Kimmeridgian, lower-Tithonan, lagoon.

الملخص

يُعد تكوين سفسيفة، الذي يعود تاريخه إلى الجوراسي الأعلى، من التكوينات الهامة المنكشفة في جبال العمور، حيث يَظهر بوضوح عند جبل الركن، جنوب غرب قرية سفسيفة، على بُعد حوالي 45 كلم شرق مدينة البيض. تهدف هذه الدراسة إلى تحليل الخصائص البيئية القديمة والتابنومية لطبقات الأصداف التي تميز هذا التكوين، وذلك لفهم أصلها وظروف ترسيبها.

تتكوَّن البنية الليثولوجية لتكوين سفسيفة من تعاقبات من المارل، وطبقات غنية بالجبس، وحجر رملي، ودولوميت، وحجر جيري أوليتي، بالإضافة إلى طبقات الأصداف الكربوناتية المميزة، والتي تُعد من أبرز الوجوه الرسوبية في هذا التكوين. وتُظهر هذه الطبقات بُنى رسوبية متنوعة، مثل التطبق المتقاطع الحوضي والأسطح التآكلية القاعدية. وقد تم تحديد مستويين غنيين بالبراكيوبودات ضمن وحدات المارل، واستُخدما كمؤشرات بيوستراتيغرافية سمحت بتأريخ التكوين إلى الكيميريدجيان المتأخر (*Xestosina arguta*)، والتي تُشير إلى الانتقال من نطاق *Eudoxus* إلى قاعدة نطاق (*Autissiodorensis*) والتيثوني المبكر (*Xestosina sera*)، التي تُمثّل نطاق *Gigas*، تحت نطاق (*Gravesiana*).

كشفت التحاليل المجهرية للمقاطع الرقيقة عن تنوّع في النُسج الكربوناتية، بما في ذلك الرودستون، والباكستون، والغراينستون، والفلاتستون، وهي نُسج تهيمن عليها بقايا الأصداف، والأووليت، والمحاريات، بالإضافة إلى حبيبات الكوارتز. وتشير هذه التغيرات، إلى جانب البُنى الرسوبية المصاحبة، إلى بيئات ترسيب بحرية ضحلة، تتراوح ما بين بيئات رمليّة متأثرة بالعواصف، إلى بيئات بحيرية مغلقة ذات طاقة منخفضة. كما تُشير البُنى مثل التطبق الحوضي، والتخريم الحيوي، ووجود طبقات جبسية، إلى تقلبات معقّدة في طاقة الترسيب وكيمياء المياه خلال الفترة الزمنية المدروسة.

تُظهر طبقات الأصداف دلائل واضحة على إعادة الترسيب والحفظ الانتقائي، مما يُشير إلى تأثير فترات طاقة عالية متقطعة في تراكمها. كما تؤكد الأدلة التابونومية، مثل تفتت الأصداف، ودرجة التحامها، واتجاهاتها، إلى جانب بيانات الميكروفاسيس، على وجود علاقة وثيقة بين العمليات الفيزيائية للترسيب وطبيعة تراكم الأصداف.

الكلمات المفتاحية: طبقات الأصداف، سفسيفة، البيض، الكيميريدجيان الأعلى، التيثوني الأسفل، بيئة بحيرية ضحلة.

TABLE OF CONTENTS

Chapter one: Generalities

I-General introduction……...…1

II- Geographic settings……...…2

II.1- General geographic settings……2

II.2- Local geographic settings……2

III- Geological settings……..…..4

III.1- Saharan atlas global geological settings……..4

III.2-Geologic setting of El Bayadh area……..7

IV- Structural settings……..10

IV.1- The Saharan atlas faults……12

IV.2- The Saharan atlas folds……13

IV.3- Major tectonic events of the Saharan atlas……....13

V- Historic of previous work……....14

VI- Material and methods……....16

Chapter two: Lithostratigraphy

I-Introduction……...18

II-Section localization……..18

III-Lithostratigraphic description……..…19

III.1- Member 01……...…19

III.2- Member 02……...19

III.3- Member 03……...21

IV-Biostratigraphic framework……21

Chapter three: Sedimentology

I -Introduction……..**28**

II- Facies inventory……..**28**

III -Sedimentary structures inventory……...**31**

IV-Carbonates rocks classification system……**36**

V-Microfacies inventory…….….**37**

VI- Discussion…….…..**46**

Chapter four: Shell beds

I -Introduction……...….**51**

I.1-How do shells concentrations form?.....**51**

I.2-Descriptive classification of shell beds…….……**52**

I.3-Genetic classification of shell beds…….……..**53**

II –Sfissifa Formation shells concentrations……...……...…….**57**

II.1–Description……...……..**57**

II.2–Taphonomic and genetic interpretation of the shell concentration……..**58**

III –Paleoenvironment synthesis……**60**

Conclusion……..…**61**



Chapter one

Generalities



I- General introduction

Historically descriptive usage of shell beds dates back to early 19th-century British mapping by (William, 1821), who applied "shell bed" to shell-rich horizons; the first formal North American formation named as a shell bed was James M. Safford's "Green Sand, or Shell Bed" in (Tennessee, 1869). Other early formal uses include Lucas Barrett's "Bowden Shell Bed" in Jamaica (circa 1862) and Cragin's "Champion Shell Bed" in (Kansas, 1895). By the late 20th century, the term had been adopted in quantitative sedimentology, exemplified by the genetic studies of shell-beds (Kidwell, 1991). Shell concentrations-accumulations of invertebrate skeletal remains larger than 2 mm in size are a widespread and significant feature in the sedimentary record. These deposits form through an interaction of many factors; biological activity, physical and chemical processes over time. These shell accumulations can be described and classified based on several key factors such as the types of organisms and their taphonomy, the internal arrangement of the skeletal remains (biofabric), their overall shape and distribution, and the level of structural complexity. Although shell concentrations are often of limited use in biostratigraphy and paleoecology due to reworking, they still retain valuable paleoenvironmental information. The deposit's fabric and the preservation state of individual shells can reveal critical and useful detail about depositional conditions and final depositional environments; Thus, genetic classifications of shell beds are more than just taxonomic exercises, they provide important insights into past sedimentary environments and help us piece together the history of basin development. This thesis presents a descriptive and taphonomic analysis of shell beds from the Sfissifa Formation, in order to: (1) decipher their genesis, (2) environmental conditions in which they formed, and (3) propose a depositional environment.

El Bayadh region is part of the central Saharan Atlas or also known as "Les Monts d'Amour" as dictate Ritter (1902) subdivision. This study took interest in the Sfissifa Formation logged SW of the Sfissifa village and east of the El Bayadh city. It consists of Upper Jurassic deposits mainly consists of marls interbedding with the shell beds with two brachiopods rich level dating the late Kimmeridgian and the lower Tithonian (Mahboubi et al., 2021), (Sadji et al., 2025).

II- Geographic settings

II.1- General geographic settings

During the Jurassic period, the Saharan Atlas was part of northwestern Gondwana, forming the southern margin of the Neotethys Ocean (Fig.01). It is now a segment of the Atlas Mountains system, which extends from Morocco to Tunisia and includes the High Atlas (Morocco), the Saharan Atlas (Algeria), and the Tunisian Atlas (Fig.02). This intracontinental mountain chain, oriented northeast-southwest, consists of Meso-Cenozoic sedimentary deposits that were deformed and uplifted during the Alpine orogeny. It spans over 1,000 km, from the Moroccan High Atlas in the west to Tunisia in the east. Situated between the Betic-Rif-Tell collision belt to the north and the West African Craton to the south, the Saharan Atlas is a significant structural feature within the Atlas system. Structurally, the Saharan Atlas is subdivided into three sections, as defined by (Ritter, 1902): the Ksour Mountains (Occidental Saharan Atlas) in the west, the Amour Mountains (Central Saharan Atlas), and the Ouled Naïl Mountains (Oriental Saharan Atlas) in the east (Fig.02). These Mountains are characterized by large scale folding and faulting, resulting from compressional forces linked to the Alpine orogeny. The Saharan Atlas is bounded to the north and south by major fault systems, which have influenced its tectonic history. Additionally, it is separated from the Tell-Rif belt to the north by the relatively stable Meseta domain, represented by the High Plateaus of Oran (Hautes Plaines Oranaises).

II.2- Local geographic settings

The study area is located within the Amour Mountains, which form the central part of the Saharan Atlas. These Mountains stretch in a SW–NE direction and are bordered by the High Plateau to the north, the Ksour Mountains (Western Saharan Atlas) to the west, the Saharan platform to the south, and the Ouled Naïl Mountains (eastern Saharan Atlas) to the east (Fig.02). The Sfissifa Formation crops out in El Bayadh area, approximately 290 km southeast of Oran city and about 45 km east of the town of El Bayadh, 200 m SW of the Sfissifa village. The Amour Mountains are composed primarily of Mesozoic and Cenozoic deposits, including siliciclastic and carbonates, along with minor marine and continental evaporitic layers. This region is characterized by a rugged landscape, with altitudes reaching up to 2,000 meters, as seen in Djebel Ksel (2008 m). The studied stratigraphic section is located at Djebel Er Roken, near the Sfissifa village (Fig.03).



Fig.01: Paleogeographic map of the Tethys ocean during the Oxfordian (158.4 ma).

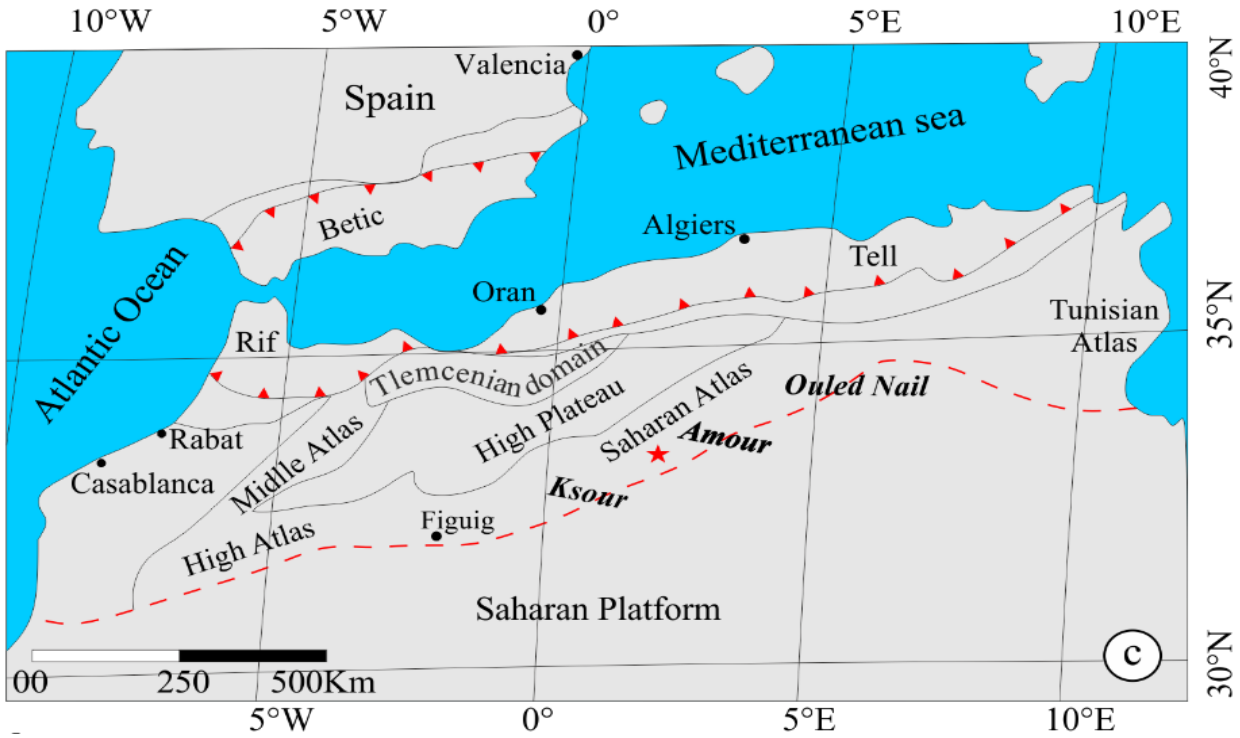


Fig.02: Geographic localization of the Saharan Atlas (Elmi, 1981).

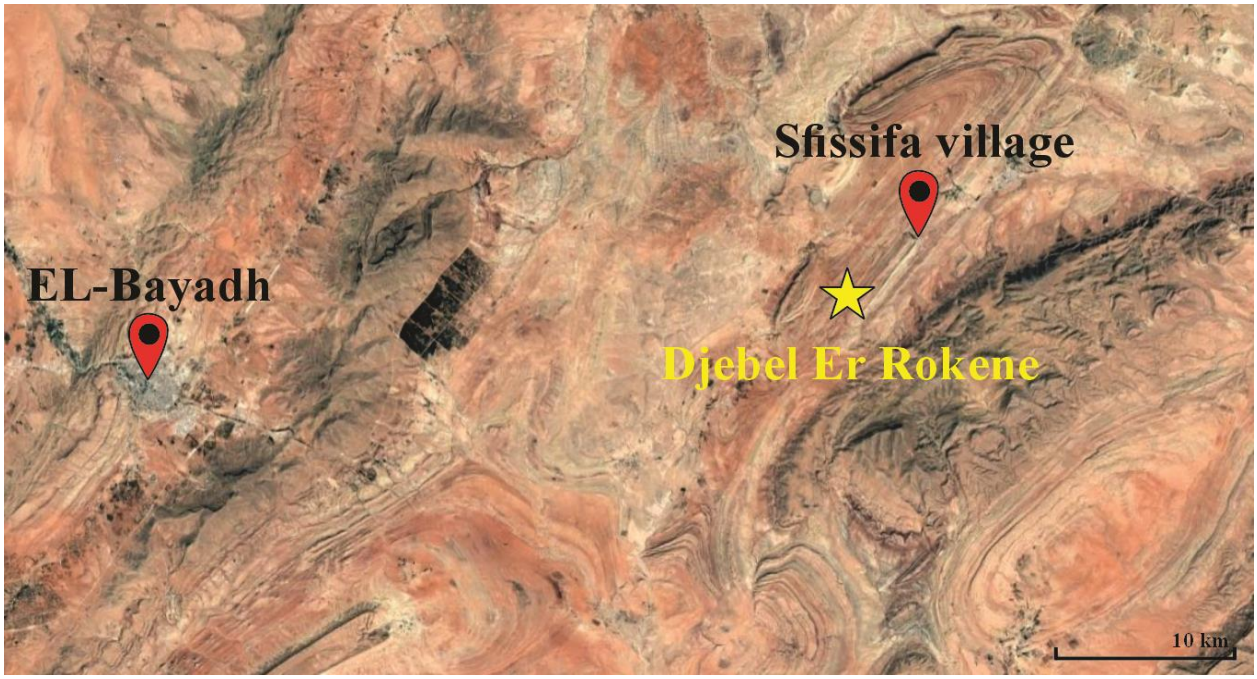


Fig.03: Satellite photography showing the localization of Dj Er Rokene (next to the Sfissifa village).

III- Geological settings

III.1- Saharan atlas global geological settings

During the Mesozoic and part of the Cenozoic, the Saharan Atlas was a site of significant marine and continental sedimentation with a thickness exceeding 10,000 meters (Emberger, 1960; Bassoullet, 1973; Douihasni, 1976; Mahboubi, 1983; Mekahli, 1995). This succession is both faulted and folded, with a predominant NE-SW structural orientation. Its formation is linked to a rifting phase associated with the opening of the Central Atlantic as in other Maghrebian basins, this tectonic evolution was influenced by the reactivation of inherited Hercynian strike-slip faults (Mattauer et al., 1977; Aït Ouali and Delfaud, 1995). Rifting and extensional activity in the basin began during the Triassic and continued through the Liassic.

The lithostratigraphic succession corresponds from bottom to top:

III.1a- Triassic

It consists of variegated gypsiferous and saline clays, with green ophitic rocks. Its originated from diapirism-related processes, displaying non conformity boundary, at the intersection of NW-SE and NE-SW faults (Meddah et al., 2007).

III.1b- Lower Jurassic

The onset of the Lower Jurassic is represented by "Formation des Dolomies de Chemarikh" of early **Hettangian** age (Mekahli, 1995). It consists of yellowish to dark gray dolomitic limestone of 130 m thick, these deposits suggest sedimentation in shallow tidal platform. (Aït Ouali, 1991).

Sinemurian to Toarcian interval is represented by two formations: the Alternance de Ain Ouarka Formation (ascribed to the Sinemurian–Pliensbachian) and the Marno-calcaire de Ain Rhezal Formation (ascribed to the Toarcian). Both formations are characterized by a marl-limestone alternations (Mekahli, 1995).

III.1c- Middle Jurassic

Aalenian–Lower Bajocian this interval corresponds to the Roknet El Kahla Formation (190 m, Aïn Ouarka), it consists of micritic limestones with lenticular oolitic breccias, and calciturbidites (Mekahli et al., 2004).

Middle–Upper Bajocian The Theniet El Klakh Formation (690 m) is a siliciclastic-carbonate unit with a lower member of laminated argillaceous sandstones, and an upper member of oolitic and bioclastic limestones interbedded with shales (Ouali Mehadji et al., 1994).

Upper Bajocian–Lower Bathonian The Tifkirt Formation (14 m thick) consists of reefal biostromes transitioning into bioherms, built by corals (*Isastrea*, *Thamnastrea*), these reefs pass into oo-bioclastic limestones with ammonites and brachiopods, providing key biostratigraphic markers (Alméras et al., 1994; Mekahli et al., 2004).

Callovian: The Kheneg Formation (Djebel Amour) represents the easternmost Jurassic deposits of the Saharan Atlas, consists of alternating shales and fine sandstones. The shales are dark to greenish and show soft-sediment deformation structures. The sandstones are thin, laminated, and include sedimentary structures like flute casts and ripples. At the top, two fossil-rich sandstone beds mark the upper boundary, indicating a deposition's break (Cornet., 1952).

III.1d- Upper Jurassic

Callovian–Oxfordian The Djara Formation in the Ksour Mountains consists of dolomites, sandstones, and clays, with increasing detrital input upward (Bassoullet, 1973; Douihasni, 1976; Kacemi, 2005, 2013). In Djebel Amour, it shows a transition into deltaic to marine sandstones and

limestones, forming the Oued El Bayadh and Theniet Et-Temar formations (Morizet, 1970; Mahboubi et al., 2021). Further east, the Ouled Naïl region records sandstones, marls, and reefal limestones (Herkat, 1982), marking a shift from terrigenous-dominated deposits in the west to carbonate-rich facies in the east.

Kimmeridgian–Tithonian The Aïssa Formation in the western Atlas is composed of argillaceous-siliciclastic deposits (Bassoullet, 1973; Douihasni, 1976). In Djebel Amour, deltaic deposits dominate, while eastern sections show more marine carbonates with oysters and algae (Morizet, 1970). The upper Oxfordian–Kimmeridgian? in Djebel Amour includes the Ksel, Laguermi, Boualem, and Sfissifa Formations (Mahboubi et al., 2021).

III.1d- Lower Cretaceous

Berriasian–Hauterivian In the western Atlas, the upper member of the **Tiloula Formation** consists of variegated sandy clays, ferruginous sandstones, and rare conglomerates, with some dolomite inclusions and copper mineralization (Kacemi, 2013; Naimi et al., 2021b). In Djebel Amour, the Valanginian (500 m) is dominated by marly limestones, while the thinner Hauterivian (150 m) starts with continental sandstones and transitions to marno-limestones (Cornet, 1952).

Barremian–Albian: The **Tiout Formation** (Ksour Mountains) is equivalent to the Saharan Continental Intercalaire and comprises three members The Tiout Formation (Barremian–Albian) consists of Lower Tiout Sandstones, reddish channelized sandstones and variegated clays, an argillaceous member red-green pelitic sediments with dolomites, gypsum, and copper minerals, and Upper Tiout sandstone-clay alternations with cross-bedding and ripple marks.

III.1e- Upper Cretaceous

Cenomanian–Turonian it corresponds, in the Ksour Mountains, to the El Rhelida Formation, this formation consists of red-green sandstones, clays, and calcarenites, rich in dinosaur footprints associated with marine fossils. Whereas, the Medaouar Formation consists of gypsum-rich layers with bioclastic limestones bears bivalve, and gastropods. The Rhoundjaïa Formation consists of carbonates with bivalves, gastropods, and rudists, showing signs of oceanic anoxic event. These formations share similarities with the Djebel Amour area (Benyoucef et al., 2017).

III.1f- Paleogene

The Paleogene deposits of the El Kohol Formation in the Djebel Amour region are known for their rich vertebrate fossils, including the first African marsupial and early species of creodonts, hyracoids, proboscidians, and bats. This formation is divided into four distinct members: a gypsum-rich transition layer, a lower red detrital layer with fossils, an intermediate marl-limestone layer containing a variety of fossil groups, and an upper red detrital layer made up of fluvial sandstones. It is scribed to the middle Ypresian age (~51-50 million years ago). The Gour formations in the area are made up of poorly consolidated debris flows, and are ascribed to the Lutetian or Miocene period (Naimi., 2022).

III.1g- Neogene\Quaternary

The continental deposits consist mainly of red clayey sandstone layers with gypsum levels of Mio-Pliocene age, typically unconformable over Barrémian-Albian sandstones. The Pliocene consists of conglomerates, limestone shells. Whereas, the travertines, ancient and recent alluvial deposits, and eolian formations, are all ascribed to the Quaternary (Naimi., 2022).

III.2-Geologic setting of El Bayadh area

The Amour Mountains are formed by a thick sedimentary deposits covering the Mesozoic-Cenozoic stratigraphic interval. While, the Triassic consists of gypsum and salt-rich clays, with local doleritic volcanic rocks. The Jurassic corresponds to carbonate rocks, marlstones and sandstone-siltstone alternations. The Lower Cretaceous is characterized by the by widespread continental sandstones known as “Continental Intercalaire”, alongside with gypsum and clay-stones. The Upper Cretaceous is composed by dolomitic limestones, gypsum-rich marls and marly-limestone alternations (Guillemot and Estorges, 1981; Abed, 1982; Kazi-Tani, 1986; Bracene, 2002; Mahboubi et al., 2007; Regagba et al., 2007; Bessedik et al., 2008). The Cenozoic is represented mainly by continental siliciclastic deposits. (Benadla et al., 2023), (Sadji et al., 2025).

Recently, (Mahboubi et al., 2021), based on two brachiopod levels, updated the lithostratigraphy of the Upper Jurassic deposits of El Bayadh area and proposed five lithostratigraphic Formations, they are from base to top: the Theniet Et-Temar, Ksel, Laguermi, Boualem, and the Sfissifa Formations. (Fig. 04).

III.1- Kheneg Formation

This formation consists of an alternation of clay and sandstone layers (Cornet, 1952). The clay beds exhibit a schistose appearance, with color ranging from grey to black, occasionally transitioning to green towards the top. These clays display soft-sediment deformation structures such as micro-slumps and olistoliths. The clays alternate with fine grained sandstone beds, of few millimeters to a several centimeters in thickness, the sandstones display greenish hue observable both on weathered surface and fresh break. The sandstones show horizontal laminations, basal scours, and sole structures like flute casts, while the upper surfaces may bear current ripples. The top of the Kheneg Formation is marked by two sandstone slabs rich in gastropods, brachiopods, and ammonites. The upper slab marks the upper boundary of this formation, corresponding to a discontinuity (Mahboubi et al., 2021).

III.2- Oued El Bayadh Formation

The type section is located on the southern flank of Djebel El-Biodh. Northeast of El Bayadh town. This formation consists of an alternation of sandstones with common sedimentary structures, clays, and dolomites. The sandstones are blackish on the weathered surface and greenish when freshly broken. Two members can be distinguished. The lower member (120 m thick) begins with green clay beds interbedded with sandstone and dolomite layers. Upward, the sandstone and dolomite beds become thicker, while the clay intervals thin out. The sandstones are fine- to medium-grained, exhibit colors ranging from pale yellow to whitish, and commonly display various sedimentary structures such as current ripples. Dolomites are yellow to grey on weathered surface, whitish on fresh break, and tend to become thicker and browner toward the top. The upper member (180 m thick) is characterized by reduced dolomite beds and thicker sandstone layers. The clays are mostly green, except for the basal levels where they are black. Sandstones occur as fine-grained, whitish beds heavily bioturbated and bearing common ripple marks. The fossil content includes broken and poorly preserved internal molds bivalves, and trace fossils. The top of this member is marked by a distinctive, 5m-thick, massive pink sandstone with clear channel features, easily recognizable in the field (Mahboubi et al., 2021).

III.3- Theniet Et-Temar Formation

The middle Oxfordian Theniet Et-Temar Formation reference section is located between Djebel Selim and Djebel Cherak, 8 km south of the Ghassoul village. This formation is characterized by a succession of alternating marl and limestone layers. The marls range from gray to black and contain spherical limestone nodules of 3 to 10 cm-sized. The limestone beds are blue to black color, vary in thickness from a few decimeters to several meters, they are partially dolomitized (Regagba. 2006). The lower and middle parts of this formation bear common fossils, including bivalves, gastropods, brachiopods, and echinoderms. Trace fossils are represented by, *Thalassinoides* and *Rhizocoralliu.* The upper part is marked by a concentration of branched corals (Mahboubi et al., 2021).

III.4- Ksel Formation

The type section is located on the northern flank of Mount Ksel 13 km northeast of El Bayadh. The base of the Ksel Formation consists of 10 m of bear barren red clay, occasionally interrupted by thin layers of reddish sandstone with dinosaur footprints. Upward, the sandstone layers become progressively thicker exhibiting cross-bedding and occasional silicified wood remains. The Ksel Formation is capped by a distinctive 5 to 7 m-thick layer of red clay, marking its upper boundary. This formation has been ascribed to the upper Oxfordian and lower Kimmeridgian without any supporting paleontological evidence.

III.5- Laguermi Formation

The reference section, located within the Laguermi valley, 15 km southeast of El Bayadh. It consists of marls interbedded with limestone layers. These limestone interbeds contain oyster shell fragments, dinosaur footprints, and crocodile bones. Followed by 70 m variegated marls of red, green, and violet, interspersed with bioclastic limestone layers ranging from 0.2 to 2 m thick, along with gypsum horizons. The top of the Laguermi Formation is marked by the appearance of massive sandstone beds. This formation has been ascribed to the upper Oxfordian and lower Kimmeridgian without any paleontological evidence in support.

III.6- Boualem Formation

The reference section is located between the Boualem villages and Sfissifa village, 44 km east of El Bayadh. It consists of massive sandstone beds ranging from 0.1 to 2 m thick, interbedded

with red to green clay layers measuring 1 to 2 m in thickness. These sandstones display various primary sedimentary structures, including flaser bedding, cross-stratification, and poorly preserved silicified wood fragments. The upper part of Boualem Formation consists of gypsum-bearing red clay. Mahboubi et al, (2021) ascribed Boualem Formation to the upper Oxfordian and lower Kimmeridgian without any supporting paleontological evidence.

III.7- Sfissifa Formation

The reference section is located at Djebel Er Roken, near the village named after it, approximately 45 km east of El-Bayadh. Sfissifa Formation is the topic of our study, and it is described in detail in chapter 2.

III.8- Continental intercalaire

It consists of 500 to 600 m of sandstone, lying between Kimmeridgian limestones and the first marly beds attributed to the Lower Cretaceous. These sandstones are stratified, heavily weathered to a black color, and exhibit ripple marks. The absence of fauna in the sandy Lower Cretaceous deposits of El Bayadh makes stratigraphic attribution a difficult task (Cornet., 1952).

IV- Structural settings

The Saharan Atlas is bounded by two major faults: the North and South Atlasic-faults. Initially interpreted by Elmi et al, (1978), the range originated from an ancient SW–NE-oriented subsiding trough situated between two stable domains: the Saharan Platform to the south and the Oranese High Plains to the north. Geologically, the Saharan Atlas is divided into a pre-Atlas zone in the north and an Atlas zone in the south (Kazi-Tani, 1986).

Structurally, the western part of the Atlas exhibits greater brittleness. Whereas, the eastern part is more ductile. The range consists of box-fold anticlines, characterized by steep limbs and nearly flat crests. These folds are short and widely spaced, forming a distinctive "procession of caterpillars" pattern (Ritter, 1902; Delfaud et al., 1974). This folding style results from Triassic evaporites, which created mechanical decoupling between the basement and overlying sedimentary cover. Diapirs are commonly associated with longitudinal thrust faults or a combination of longitudinal and transverse strike-slip faults (Douihasni, 1976).

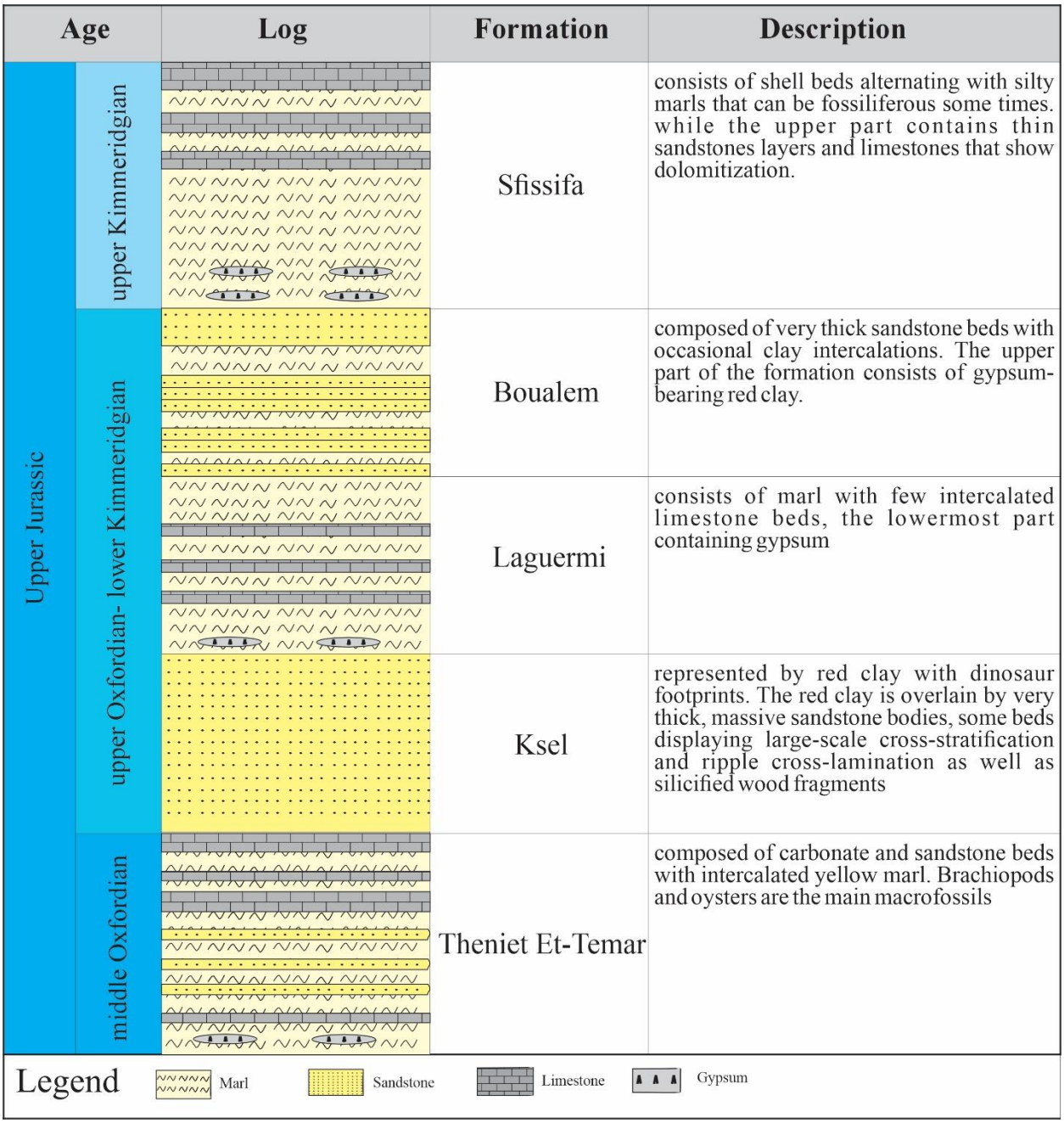


Fig.04: Log synthetizing the Late Jurassic formations of El Bayadh region.

IV.1- The Saharan atlas faults

a-North Atlasic-fault

It is a discontinuous tectonic feature with a quick change in direction. This fault runs from the northeast of El-Bayadh to the north of Aflou in the central Saharan Atlas, with a direction changing from Northeast/Southwest to East/West near Bou Saada. It extends from Bou Arfa in Morocco to Zahrez Chergui in Algerian, separating the less deformed pre-atlasic domain from the folded atlas. This fault is sometimes confused with the Southern Mesetian Fault (Guiraud., 1973).

b-South Atlasic fault

It corresponds to a chain of faults that generally run in an ENE-WSW direction. It stretches for about 2000 km, from Agadir in Morocco to the Gulf of Gabès in Tunisia separating the relatively stable Saharan region from the folded Atlas region (Guiraud., 1973).

c-Transversal fault

Elmi, (1978) highlighted six transversal faults as showed in (Fig.05):

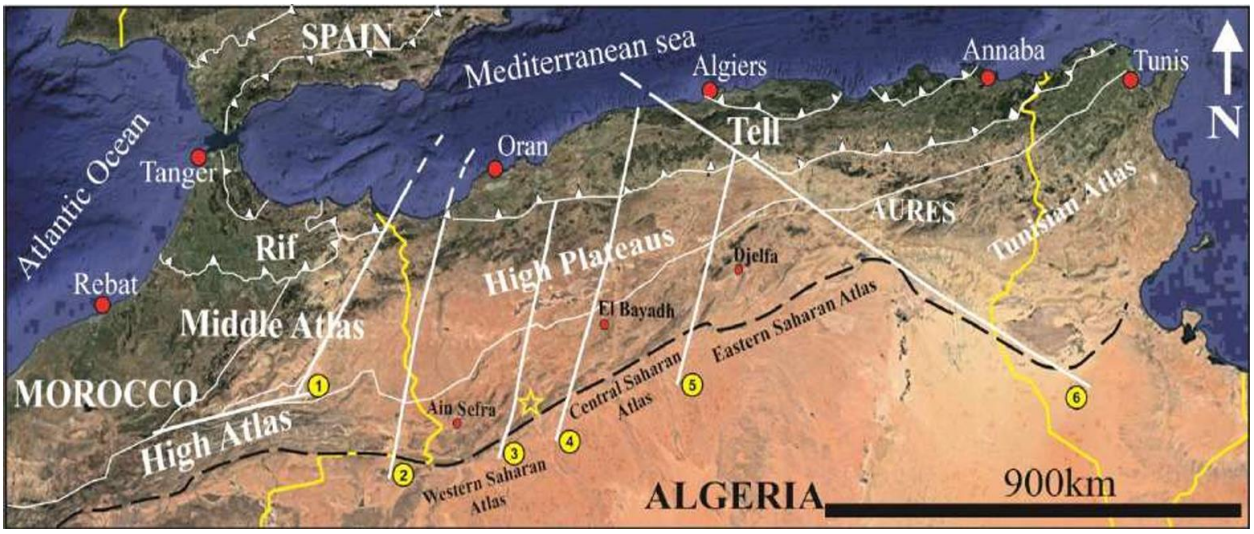


Fig.05: Map of the north Africa showing the main structural features of the Atlas 1. Transversal of the Moulouya ; 2. Transversal of the Tafna-Magoura ; 3. Transversal of the Ain Séfra – Saida; 4. Transversal of the El-Bayadh- Tiaret; 5. Transversal of the Theniet El Had; 6. Transversal of the Aurès – Hodna (Elmi, 1978 edited by Mahboubi et al., 2021b).

IV.2- The Saharan atlas folds

The Saharan Atlas is characterized by large scale folds (Jurassic-style) oriented N40 to N50 relative to the N60 direction of the Atlas range (Nouar, 1992). The anticlines, with Middle to Upper Jurassic cores, are long and narrow, featuring steep flanks and flat crests (Kazi-Tani, 1986). They often appear in a stepped arrangement and are frequently affected by faults with orthogonal orientations and variable displacements. Some of these faults have allowed Triassic plastic series to reach the surface at the cores of certain anticlines. The anticlines are separated by wide, basin-like synclines that interconnect, giving the region a thrust-fold style (Kazi-Tani, 1986). These NE-SW-oriented synclinal basins have Upper Cretaceous cores (Mahboubi, 2021).

IV.3- Major tectonic events of the Saharan atlas

Based on the most recent papers documenting about the Saharan Atlas (Kazi Tani, 1986; Mahboubi., 2021; Naimi, 2022) it can be synthesized into six major phases that shaped and structured the atlasic chains as they are actually:

a-Eo-Cimmerian Phase (Triassic-Jurassic boundary): Marked by extensional forces due to the opening of the Neo-Tethys Ocean and the Central Atlantic. This phase led to the formation of subsiding Mesozoic basins and the emplacement of magmatic rocks.

b-Neo-Cimmerian Phase (Middle Berriasian): Characterized by the formation of upright concentric folds oriented N10°-N20° and faults trending N60°-N80°.

c- Emscherian or Laramian Phase (Turonian-Senonian): Led to the development of NW-SE folds, which are well-represented in the Saharan Atlas.

d- Atlas Phase (Middle Eocene-Lutetian): it is the most significant tectonic phase, progressively shaping the Atlas structure from the second half of the Eocene. It produced NE-SW folds and faults trending NE-SW, NW-SE, and E-W. It is characterized by thick layers of breccias and conglomerates on their substrate and have been ascribed without paleontological evidence to the middle to upper Lutetian. Most triassic diapirs were exposed at the surface as a result of this tectonic phase.

e- Mio-Pliocene Phase: A major compressive phase affecting the entire Atlas, responsible for E-W folds in the central Saharan Atlas and structural adjustments along the South Atlas Fault. This phase largely influenced the current structure of the fault.

f- Quaternary Phase: a compressive event primarily affecting the eastern Saharan Atlas.

V- Historic of previous work

Since the 19th century the Saharan Atlas was a subject to multiple geological researches. The central part (Amour mounts) of the Saharan Atlas draws a fair geologist's attention. The Saharan Atlas has been studied essentially for their paleontological, structural and sedimentological aspects as well as cartography.

1-Exploration period (1857-1911)

Between 1850 and 1911, geologists including A. Pomel, A. Peron, G. Cotteau, and E.Ritter, dedicated their research to the stratigraphy of northern Algeria. A major milestone was reached in 1889 with the publication of the first geological synthesis at a scale of 1/800,000 by Pomel and Pouyanne. This era also saw significant advancements in understanding Algeria's geological structure, particularly the tectonic aspect, as highlighted by the works of Ficheur (1883-1897).

For the Central Saharan Atlas in 1857, de Colomb and Dr. Mares conducted a survey along the southern flank of the Saharan Atlas, traveling from El Abiodh Sidi Cheikh to the Kenadsa Zaouïa via Figuig. de Colomb focused on meteorological and topographical observations, while Mares identified the sandstones near El-Bayadh as belonging to the Lower Cretaceous.

Pouyanne and Perron (1874-1883) mapped the Cretaceous formations in the El-Bayadh region.

E. Ritter's 1902 publication, which provided crucial insights into the region's stratigraphy. Another key contribution came in 1911 from G.B.M. Flamand, whose research focused on Djebel Amour and remains a reference for the area's geological framework.

2- Second period (1911-1952)

The Central Saharan Atlas drew increased attention, notably through the detailed work of R. Lafitte (1939–1949). In preparation for the 1952 International Geological Congress in Algiers, several studies were carried out, resulting in the publication of a 1\500,000 geological map of Algeria.

<table>
<tr><th colspan="2">Regagba (2006) subdivision</th><th colspan="2">Mahboubi (2021) subdivision later modified by Sadji (2025)</th></tr>
<tr><th>Formation</th><th>Age</th><th>Formation</th><th>Age</th></tr>
<tr><td rowspan="3">Tiloula</td><td rowspan="3">Valanginian \ Hautervian</td><td>Sfissifa</td><td>lower Tithonian</td></tr>
<tr><td rowspan="2">Sfissifa</td><td>upper Kimmeridgian</td></tr>
<tr><td>Boualem</td><td rowspan="3">upper Oxfordian– lower Kimmeridgian</td></tr>
<tr><td rowspan="2">Aissa</td><td rowspan="2">Upper Jurassic</td><td>Laguermi</td></tr>
<tr><td>Ksel</td></tr>
<tr><td rowspan="2">Theniet Et Tamar</td><td rowspan="2">upper Oxfordian– lower Kimmeridgian</td><td>Theniet Et Ttamar</td><td>middle Oxfordian</td></tr>
<tr><td>Djara</td><td>Callovian-Oxfordian</td><td>Oued el bayadh</td><td>lower Callovian-lower Oxfordian</td></tr>
<tr><td>Theniet El Kelakh</td><td>lower Bathonien-lower Callovian</td><td>Kheneg</td><td>lower Callovian</td></tr>
</table>

Table.01 comparison between the old and new subdivision of the upper Jurassic of El Bayadh.

3- Third period (1952-1973)

Cornet (1952) mapped the Central Saharan Atlas, while Emberger (1960) outlined the geology of the eastern Ouled Naïl Mountains. Bassoulet (1966–1973), especially his thesis (1973), was a key to understanding the Mesozoic of the Ksour Mountains. Studies by Caratini (1968), Guiraud (1973), Bassetto and Coumes (1967), and Kazi Tani (1970) refined sedimentary and structural knowledge in the Bou Saâda area. From 1945 to 1965, SN REPAL carried out geological surveys, and SONATRACH followed with borehole drilling in 1964–1965 around Azreg (Laghouat) and Aïn Madhi, contributing to subsurface and petroleum research.

4-Modern period (from 1973)

Geological maps at 1\200,000 scale covered areas like Aïn Rich, Brézina, Laghouat, and El Bayadh, under the direction of D. Bassetto and J. Guillemot. SONATRACH later carried out more detailed 1\50,000 surveys, improving knowledge of regional stratigraphy and structures. J. Delfaud (1974) proposed a sedimentary model for the area's continental units, while M. Herkat provided an important contribution to stratigraphy and sedimentology of this region. More recently, A. Bettahar and N. Benkerrou have studied major faults and tectonics. Jurassic sequences of Djebel Amour were studied by S. Abed (1982)**,** with Kazi-Tani (1986) analyzing the Jurassic–Cretaceous transition. M. Mahboubi (1983–1990) focused on the Upper Cretaceous and Tertiary formations. Nouar (1992) introduced remote sensing to study Djebel Amour's structure, and Regagba (2006) examined the Middle and Upper Jurassic around El Bayadh. Maameri (2007–2018) worked on dinosaur footprints from the Late Triassic to the Cenomanian, contributing to ichnology and paleobiogeography. Most recently, Mahboubi (2021) studied fluid migration and diagenesis of the Jurassic formations at Aïn Ouarka and El Bayadh.

VI- Material and methods

VI.1-Bibliography

This study based on previously published data including thesis and papers dealing with the Mesozoic deposits of the central Saharan Atlas (Regageba, 2006; Mahboubi, 2021; Sadji et al., 2025).

VI.2-Field work and sampling

Exposed Upper Jurassic rocks of the El Bayadh area consist to a large extent of marine deposits (Theniet Et-Temar, Laguermi, and Sfissifa Formations). At N 33°42'05", E 1°28'29" (1373 m), the Sfissifa Formation yielded abundant oysters and brachiopods. Two One representative section from the Sfissifa Formation was measured bed-by-bed in order to shed light on the depositional environment. Rock samples were collected for microfacies analysis. Additionally, oyster and brachiopod specimens were collected.

VI.3-Laboratory work

Twenty thin-sections were made from rock and fossil samples of the Sfissifa Formation The thin-sections of rock samples and oysters were examined and photographed using a Zeiss

Axiocam 506 color microscopy digital camera (*GeoZentrum* Nordbayern, Erlangen, Germany). These data were provided by Mr. SADJI as part of a project on Mesozoic carbonate deposits in Western Algeria.

Chapter two

Lithostratigraphy

I-Introduction

This chapter presents a lithostratigraphic description of the Sfissifa Formation, based on field studies conducted during two missions near the village of Sfissifa, located east of the El Bayadh city. The Sfissifa Formation is mainly characterized by shell beds and marls, as initially described by (Mahboubi et al., 2021a), and later refined and revised by (Sadji et al., 2025) who delineated the limit Kimmeridgian-Tithonian within this Formation, while taking in consideration various sedimentological aspects such sedimentary structures, and paleontological characteristics. The established biostratigraphic framework proposed by (Sadji et al., 2025) relies on brachiopod fauna collected from two marl-rich levels, as described and detailed in the following sections.

II-Section 01

II.1-Section localization

The studied section of Sfissifa Formation, approximately 95m thick was logged bed by bed 200 m SW of the Sfissifa village (Fig.06) (coordinates: 33°42'05" N, 1°28'29" E; altitude: 1373 m), extending southward to up to the National Road No. 47. The section can be easily distinguished by its thick gypsum beds and abundant thick shell beds.

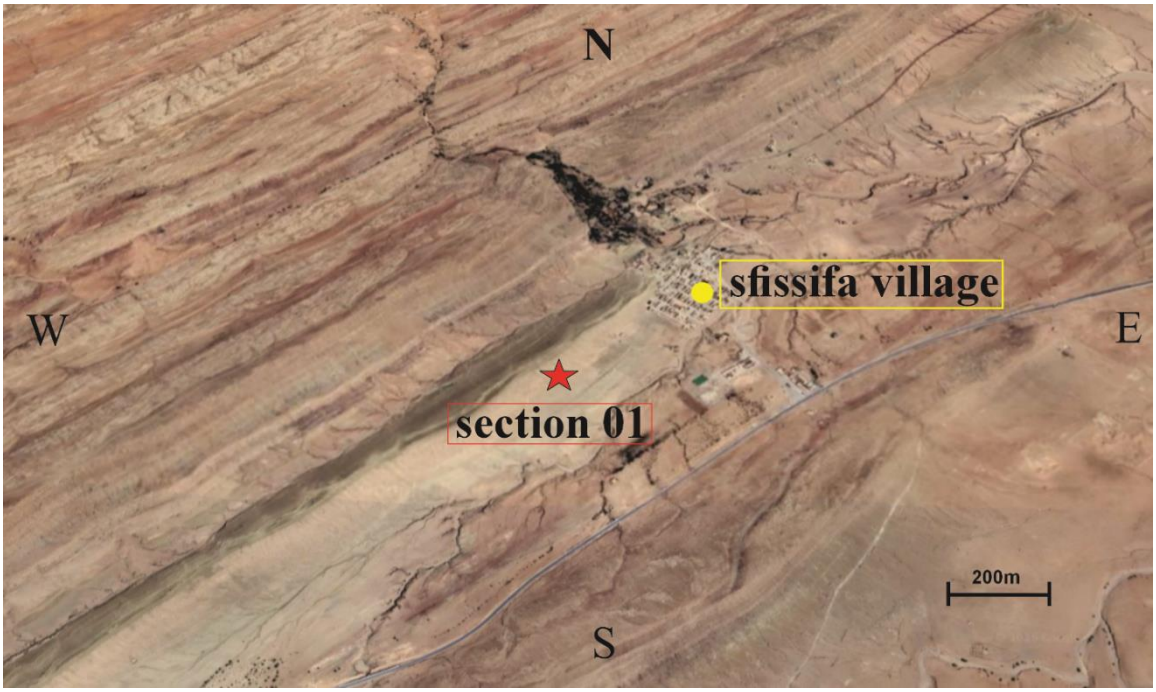


Fig.06: Google earth image showing the localization of the Sfissifa outcrop section, the red star marks the beginning of the section.

II.2-Lithostratigraphic description

The studied Sfissifa Formation, underlain by the upper Oxfordian and lower Kimmeridgian (?) Boualem Formations and overlain by the well-known "Continental Interclaire" (Fig.8A) consists mainly of carbonate deposits with minor siliciclastic intercalations. Macrofossils assemblages are dominated by oysters and brachiopods, associated with rare gastropods and echinoids. Based on lithological and paleontological criteria, the Sfissifa Formation can be subdivided into three members as detailed in the following sections.

II.2.a- Member 01

The first member begins with a distinctive basal interval composed of alternating white and dark gypsum beds (Fig.8B), each ranging from a few centimeters to several decimeters in thickness. This gypsum-rich unit, reaching a total thickness of approximately 1.5 meters, directly overlies the continental sandstones of the Boualem Formation. Above the gypsum lies a thick succession of yellow to green marls containing numerous gypsum lenses, typically 0.5 to 1 meter thick. No macrofossils have been observed in the lower portion of the member, rendering it a barren interval.

II.2.b- Member 02

This member consists of an alternating bioclastic limestone and marl 32 m thick. The bioclastic limestone beds (shell beds) ranging from 5 to 50 cm in thickness, and are predominantly composed of oysters remains.

The base of this member corresponds to the first occurrence of a very thick bioclastic limestone bed. This bioclastic limestone comprises a succession of yellowish limestone layers (Fig.8D), easily distinguishable in outcrop due to their color and massive appearance. Laterally, this thick bioclastic limestone bed varies in thickness from 1 to 2 m-thick. This bed consists of a mixture of disarticulated and fragmented oyster shells (Fig.8E), with sporadic brachiopods and rare gastropods. Some of the beds within this interval are oolitic frequently containing a mixture of ooids and shell debris. The contact between the marl and the overlying limestone corresponds to a sharp and irregular boundary (Fig.8F). The limestone beds bear abundant sedimentary structures, among them trough cross-bedding (Fig.9A) and parallel laminations (Fig.9B).

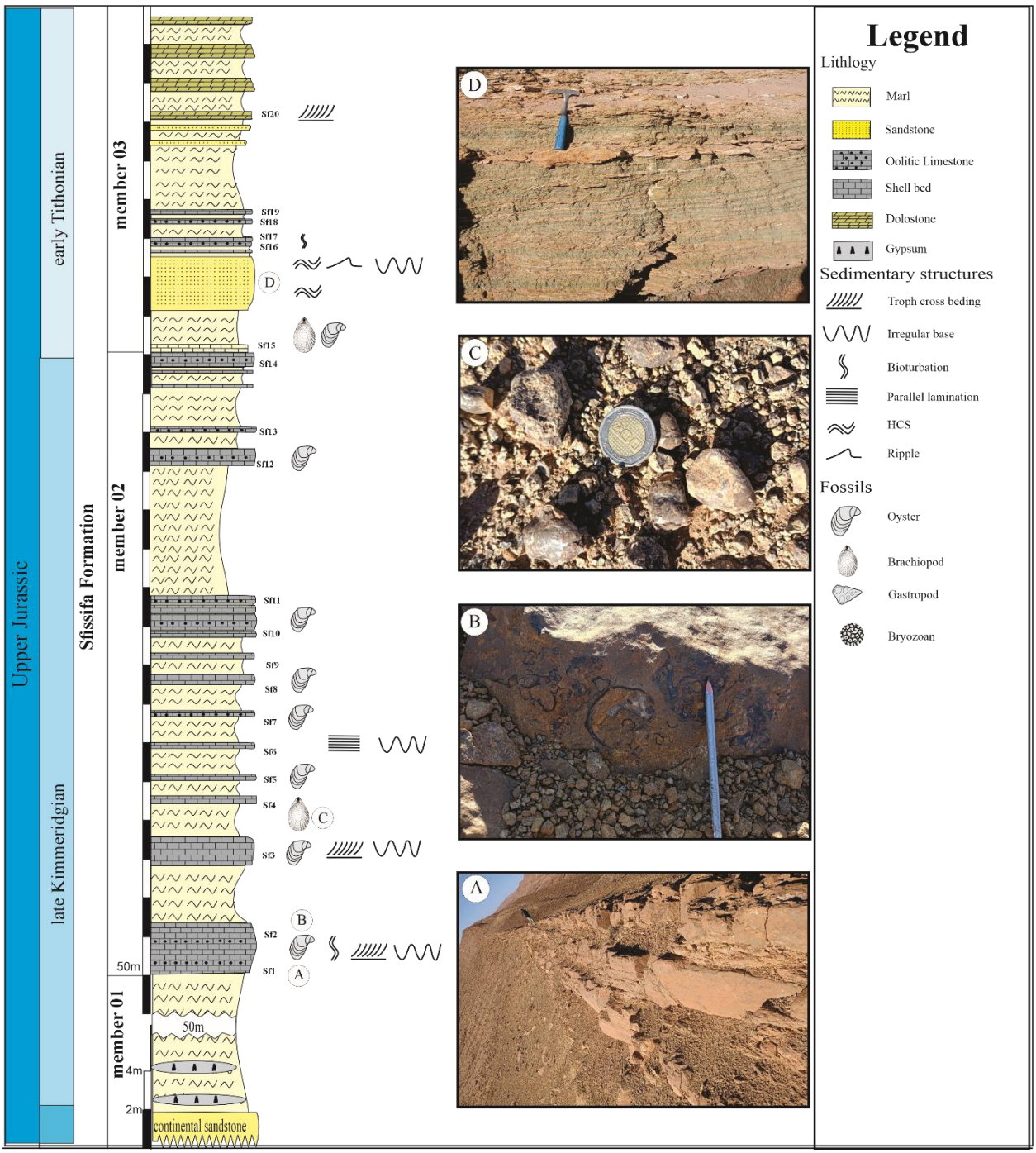


Fig.07: Lithostratigraphic log of the Sfissifa Formation. **(A)** The first carbonates bed of the second member (Shoal). **(B)** Disarticulated oyster shells. **(C)** Brachiopods fossils in silty marls (the first brachiopods level). **(D)** Sandstone-marl alternation and the first terrigenous deposits of the Sfissifa Formation.

Whereas, the marl intervals vary between few centimeters and 6m. The first marl interval bears abundant brachiopod-rich level (Fig.8C). This brachiopod level corresponds to a monospecific assemblage exclusively represented by the genus *Xestosina arguta* dating the early Kimmeridgian. This member also is characterized by the presence of new to science oyster genus *Pseudexogyra euryhalina* n. gen. et n. sp (Fig.12A).

II.2.b- Member 03

This member starts with the second marl unit, which bears a second brachiopod-rich level represented by the genus *Xestosina sera* (Fig.9C), this level marks the upper boundary of the second member and the onset of early Tithonian deposition. The third member represents the only interval within the Sfissifa Formation dominated by terrigenous input. It is composed of a package of alternating marl and sandstone layers, commonly exhibiting sedimentary structures such as hummocky cross-stratification (HCS) (Fig.9D) and languid ripple marks (Fig.9E). The marls display a gradual color shift, transitioning to a more greenish color (Fig.9F) compared to the underlying units. Notably, this entire package is devoid of macrofossils. Overlying this siliciclastic dominated interval is a highly bioturbated oolitic limestone bed, characterized by intense horizontal burrowing (Fig.9G). The trace fossils are well-developed and dense, indicating a temporary reduction in terrigenous input.

The member continues above the oolitic limestone with additional alternations of sandstone and marl layers. The top of the third member is characterized by dolostone beds and partially dolomitized shell beds intercalated with marl layers. The dolostone is typically massive to thick-bedded (Fig.9H), and frequently often exhibits trough cross-bedding along with erosional bases (Fig.9H). The interbedded marls are mostly unfossiliferous, although some layers contain scattered, well-preserved oyster shells, typically whole specimens. These fossil occurrences are rare compared to the underlying members. Finally, The Sfissifa Formation is conformably overlain by a very thick sandstone unit representing the lower Cretaceous “Continental Intercalaire”.

II.3-Biostratigraphic framework

The Sfissifa Formation was initially ascribed to the upper Kimmeridgian (Mahboubi et al., 2021) based on one brachiopod level represented by the *Xestosina arguta* (*Eudoxus* zone to *Autissiodorensis* zone). However, the second level of brachiopod which is composed solely of the genus *Xestosina sera* allowed us to ascribe the third member to the early Tithonian (*Gigas* Zone

(*Gravesiana* Subzone) (Sadji et al., 2025). Notably, this represents the first documented occurrence of *Xestosina sera* representing the *Gigas* Zone (*Gravesiana* Subzone in Africa, Consequently, we propose revising the age of the Sfissifa Formation to the late Kimmeridgian and early Tithonian.

The classification of the brachiopods is based on Williams et al. (1996), presented in the revised edition of the Treatise on Invertebrate Paleontology concerning rhynchonellide brachiopods (Lee et al., 2006).

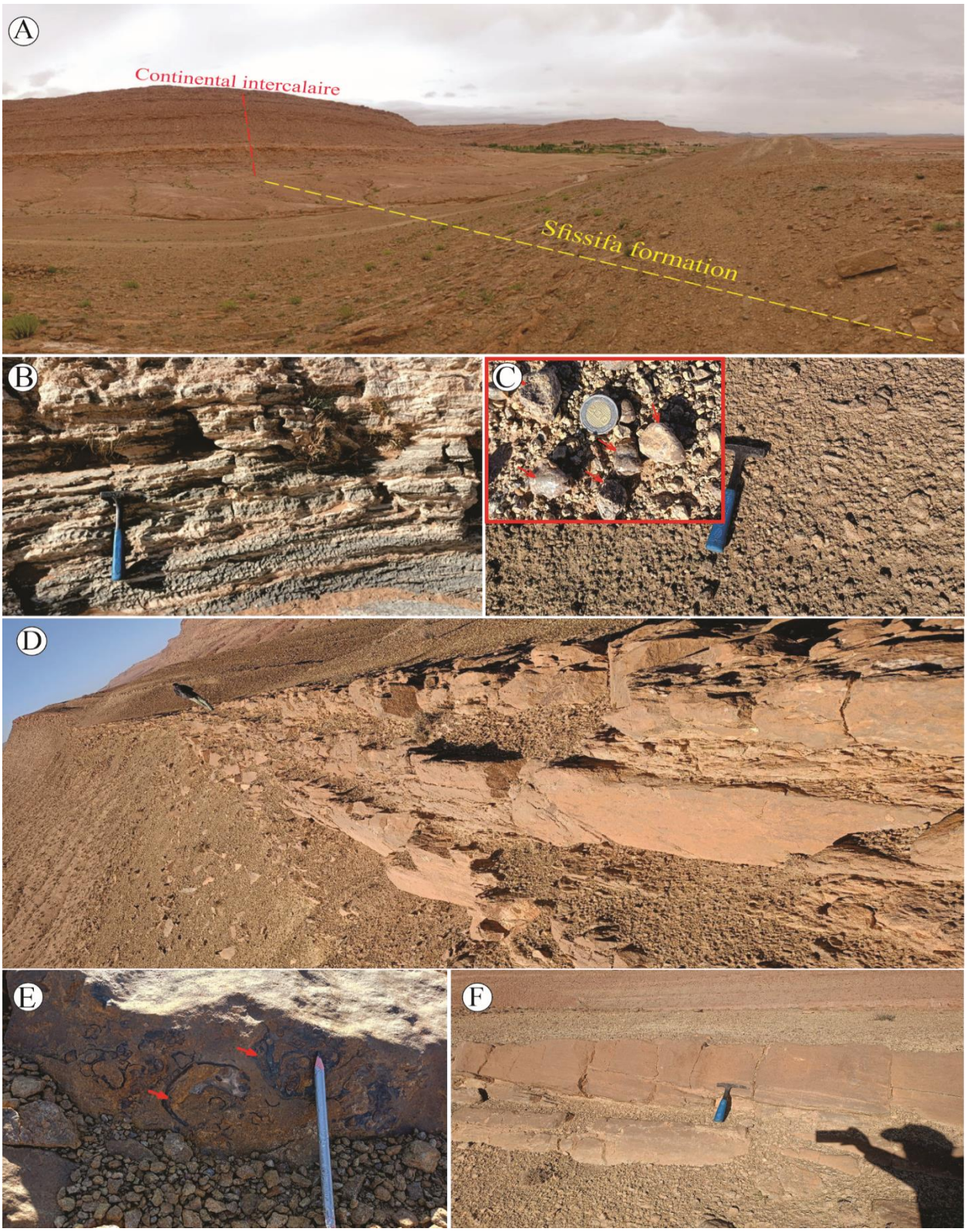


Fig.08: (A) Panoramic photograph showing the Sfissifa Formation and the Continental Intercalaire**; (B)** Alternating of white and dark gypsum layers; **(C)** First brachiopods level with a close up view**; (D)** Massive package of limestones with shell beds intercalation**; (E)** Cemented oysters shells**; (F)** Erosive base below limestone bed.

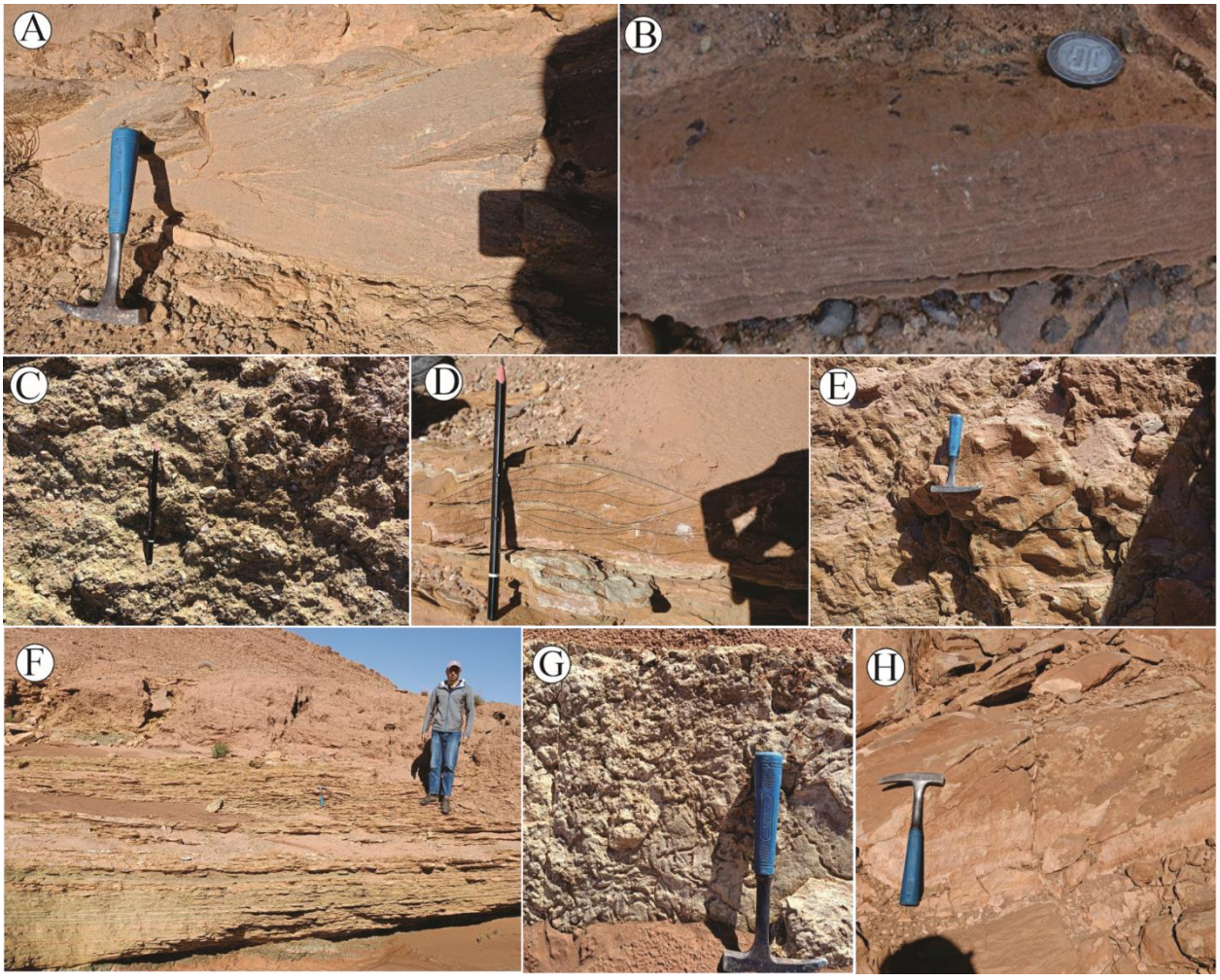


Fig.09: (A): Trough cross-beddings**; (B)** Parallel laminations**; (C)** Second brachiopod level; **(D)** HCS; **(E)** Languid ripples; **(F)** Alternating sandstone layers with green marls; **(G)** Bioturbated oolitic limestone; **(H)** Massive dolostone beds.

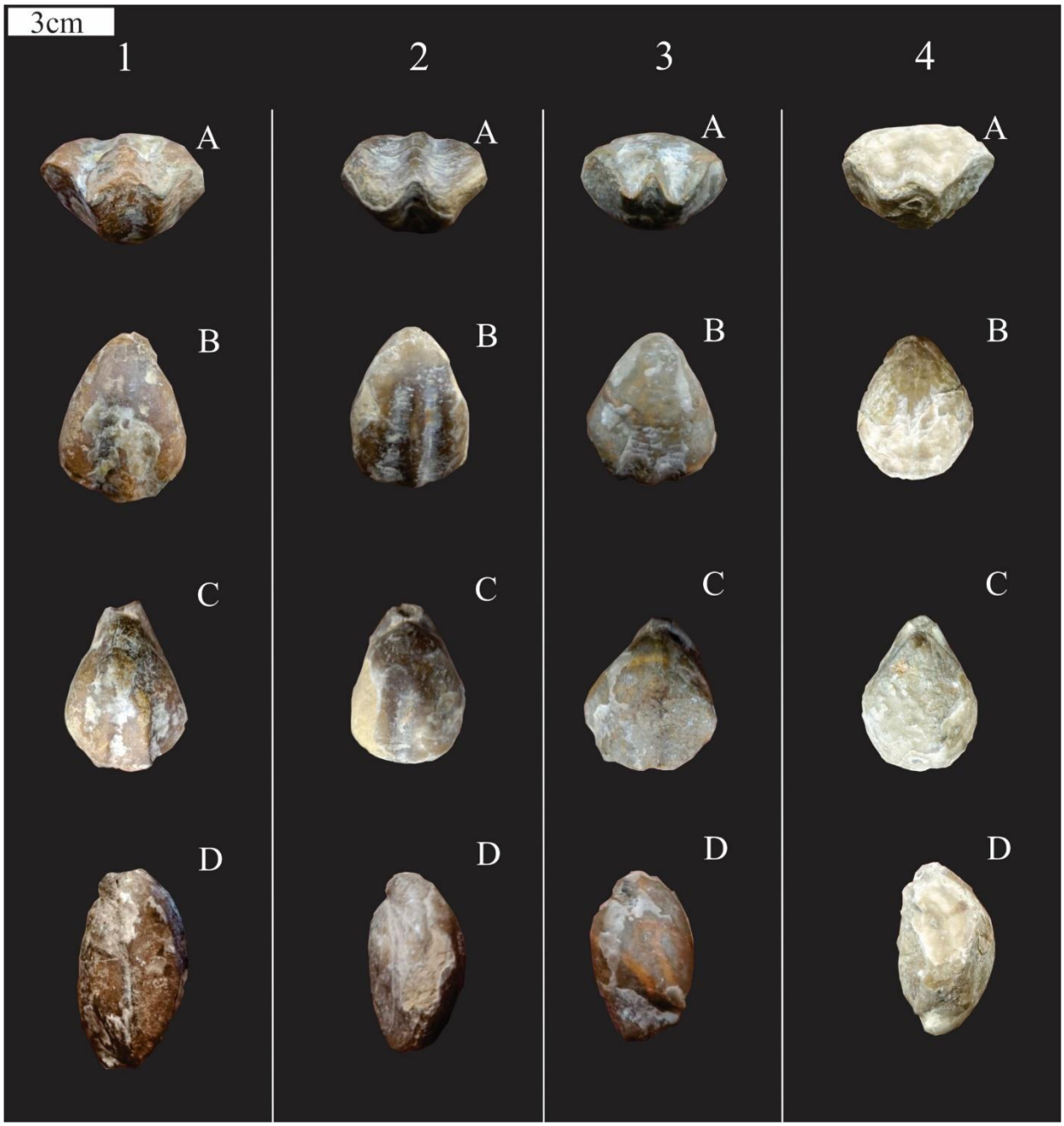


Fig.10: Upper Kimmeridgian *Xestosina arguta* (transition from the *Eudoxus* Zone to base of the *Autissiodorensis* Zone), Djebel El Roken, El Bayadh area, Sfissifa Formation. dorsal **B**, ventral **C**, lateral **D**, and front **A** views. (scale 3cm). (member 01, 50m).



Fig.11: early Tithonian *Xestosina sera* representing the *Gigas* Zone (*Gravesiana* Subzone), Djebel El Roken, El Bayadh area, Sfissifa Formation. dorsal **B**, ventral **C**, lateral **D**, and front **A** views. (scale 3cm). (member 02, 81m).

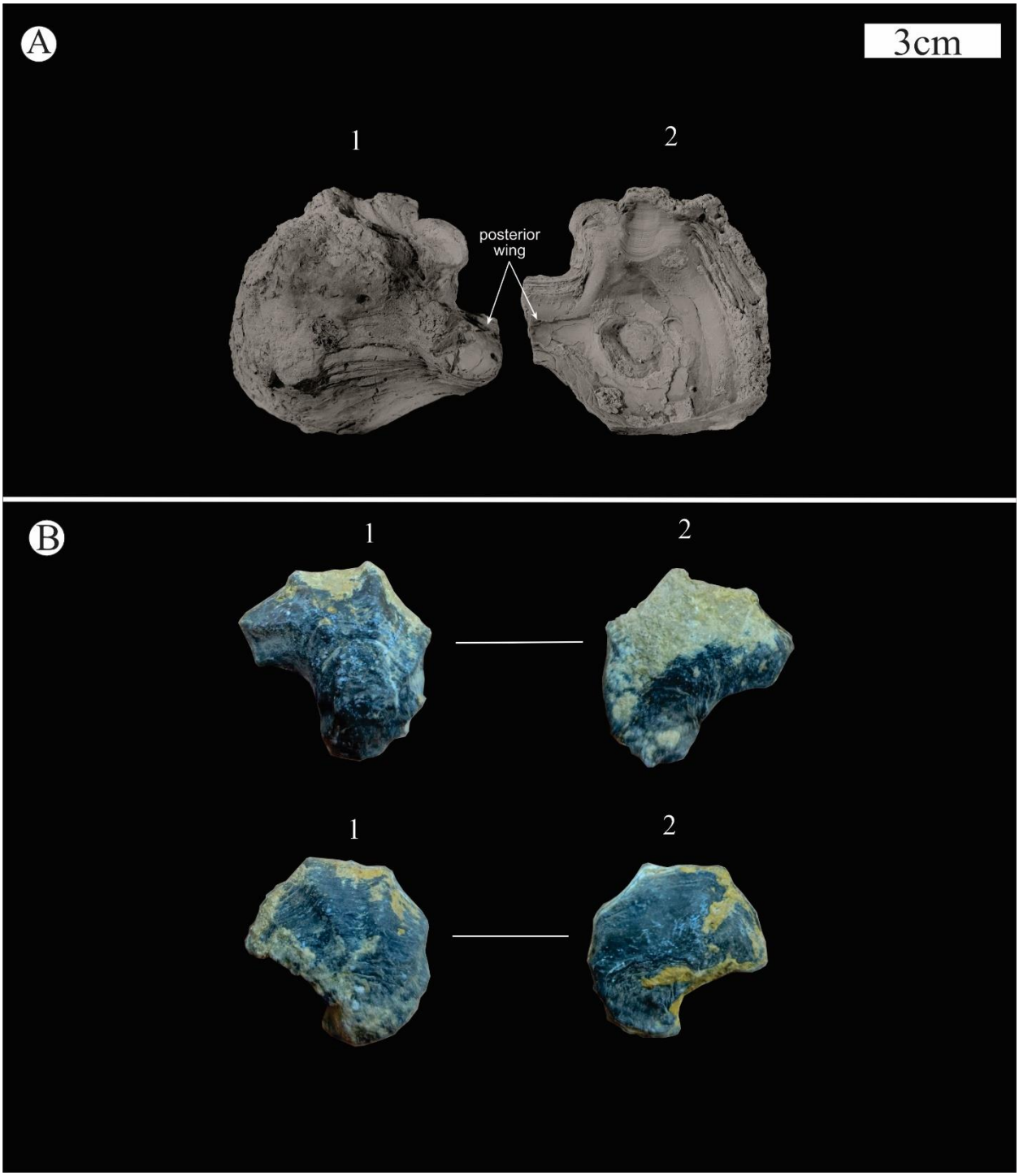


Fig.12: A: Upper Jurassic oysters: *Africogryphaea geniculata* n. sp (member 02, 53m). **B:** *Pseudexogyra euryhalina* n. gen. and n. sp (membre 3), dorsal **2**, ventral **1**. (scale 3cm). (and Djebel El Roken, El Bayadh area, Sfissifa Formation).

Chapter three

Sedimentology

I -Introduction

This chapter provides a detailed exploration of various sedimentological aspects of the Sfissifa Formation. It begins with the identification and interpretation of the different facies present within this Formation, followed by a comprehensive inventory of the observed sedimentary structures. Finally, it displays a detailed microfacies analysis of limestones and carbonate-based shell beds, aiming to collect and interpret the maximum possible data. Ultimately, the collected data from sedimentary structures, facies, and microfacies, will be synthesized in order to develop a refined paleoenvironmental reconstruction of the Sfissifa Formation. (a table for facies and microfacies abbreviation is provided in the end of the chapter).

II- Facies inventory

A-Facies A: Shell beds

1-Description

The shell beds of the Sfissifa Formation constitute the second dominant and most characteristic facies throughout the Formation, exclusively in a carbonate dominated system with centimetric thicknesses (Fig.13A-B) varying from a few centimeters to 50 cm bearing some currents sedimentary structures as trough cross-beddings.

2-Interpretation:

Dense accumulations of bioclasts can be generated in several sedimentary environments (fluvial, lacustrine, transitional, or marine) by physical\chemical, or biological processes (Kid well et al., 1986; Fürsich and Oschmann, 1993., Rodriguez et al., 2022).

(Further information, including taphonomic data and interpretations of the shell beds, see Chapter 4).

B-Facies B: Oolitic limestones

1-Description

The oolitic limestone is the third most dominant facies in Sfissifa Formation, it appears dominantly structureless and massive beds, thickness vary from few centimeters to 30 cm maximum (Fig.13C). They appear brownish on both fresh and weathered surfaces and can be white to grey in the third member. They display multiple sedimentary structures such as trough cross-beddings, parallel laminations and erosive basal surfaces while the beds located just after the HCS

sandstones are characterized by an intense bioturbation (any microfacies data of the limestones component will be given in detail further in this chapter).

2-Interpretation

Oolitic limestones are generally considered to form in shallow high-energy environments, such as the inner ramp and carbonate banks (Flugel, 2010). However, some studies have reported their presence in relatively low-energy settings, which have been described as intermittent high-energy environments (Zhang et al., 2020). Similarly, in this study, the depositional environment of oolitic limestones in the Sfissifa Formation could also be interpreted as an intermittent high-energy environment. The oolitic limestone in the Sfissifa Formation believed to be deposited in shallow-water environment as shoal deposits for the oolitic limestone of the second member and intertidal environment for the third member).

C-Facies C: Dolostone

1-Description

The upper part of the Sfissifa Formation is characterized by the third member, which consists of massive (Fig.13D) centimetric to metric scale dolostone beds varying from 15cm to approximately 1m displaying a yellow color on both fresh and weathered surfaces. Some beds exhibit sharp boundaries with the underlying marls, forming irregular basal contacts, while others have abundant trough cross-beddings.

2-Interpretation

The dolostone present in the Sfissifa Formation can be considered as a secondary dolostone, formed through post-depositional dolomitization (e.g., Folk and Land, 1975), which alters the original limestone fabric. This is evident in our dolostone, where dolomitized shells and carbonate matrix can be observed (Fig.17M). In arid coastal settings, such as modern sabkhas, high evaporation rates cause the precipitation of evaporites and the formation of Mg-rich brines. These brines infiltrate the underlying carbonate sediments, replacing calcite with dolomite (Warren, 2000).

D-Facies D: Sandstone

1-Description

In the Sfissifa Formation, pure terrigenous sedimentation is relatively rare and occurs mainly in the third member, just after the Kimmeridgian-Tithonian boundary. Here, thickening-upward centimetric with medium sized grains sandstones layers alternate with greenish-colored marls. The sandstones often exhibit hydrodynamic sedimentary structures on both their interfaces and epirelief such as: HCS, parallel lamination and ripple marks.

2-Interpretation

Terrigenous sediment supply is often linked to high stand or regressive phases, there presence within a carbonate succession can also indicate tectonic activity, such as uplift and erosion of nearby landmasses, or variations in sea level that alter sediment supply (Catuneanu, 2006). The sedimentary structures reflect high hydrodynamic energy during the depositional process.

E-Facies E: Silty marls

1-Description

The marls in thee Sfissifa Formation is most likely carbonates riche due to the high carbonates deposits around it. Mixed with silty sized siliciclastic particles, and predominantly yellow in color. They are mostly unfossiliferous except for two distinct brachiopods rich levels. In the second brachiopod levels marls show a transition to a more greenish color.

2-Interpretation

Marls typically form in low-energy settings and can occur in various environments where fine-grained carbonates and clay settle from suspension (Tuker., 1991). The two brachiopod-rich levels, in contrast to the otherwise unfossiliferous marls, suggest a temporary increase in oxygenation or nutrient input that allowed brachiopods to thrive. These conditions could correspond to a sea-level fluctuation **(**Brett and Baird, 1986**).**

F-Facies F: Gypsum

1-Description

In the base of the first member from the Sfissifa Formation gypsum can be encountered under two forms. Firstly, they can be seen as centimetric parallel layers alternating with marls (Fig.13E), and the other form is as lenses or lenticular bodies, often dispersed throughout marls. They vary in size from a few millimeters to several centimeters and can occur as isolated Lense shape or thin, discontinuous layers parallel to bedding.

2-Interpretation

Laminated evaporites indicate uniform depositional conditions over a broad area. Laminites are commonly interpreted as forming through the precipitation of evaporites in calm water below the wave base. They likely develop either in shallow-water environments protected from strong bottom currents and wave agitation or in deeper water settings (Boggs, 2006). The occurrence of gypsum lenses in marls suggests episodic restriction of marine or lagoonal waters, where periods of increased evaporation promoted sulfate precipitation. The alignment of gypsum lenses parallel to bedding implies precipitation in low-energy, subaqueous conditions with limited disturbance. (Schreiber and Tabakh, 2000).

III -Sedimentary structures inventory

A-Hummocky cross-stratifications (HCS)

1-Description

In the Sfissifa Formation, hummocky cross-stratification is exclusively observed within the sandstone package in the third member of the succession. It occurs in sand beds interlayered with green colored marls. This sedimentary structure appears at a centimetric scale, with an average thickness of approximately 15 cm, displaying multiple sets of convex-up and concave-up laminae stacked vertically (Fig.14A-H). These sets exhibit lateral continuity, maintaining a consistent geometric pattern. The individual sets are separated by be sharp boundaries.

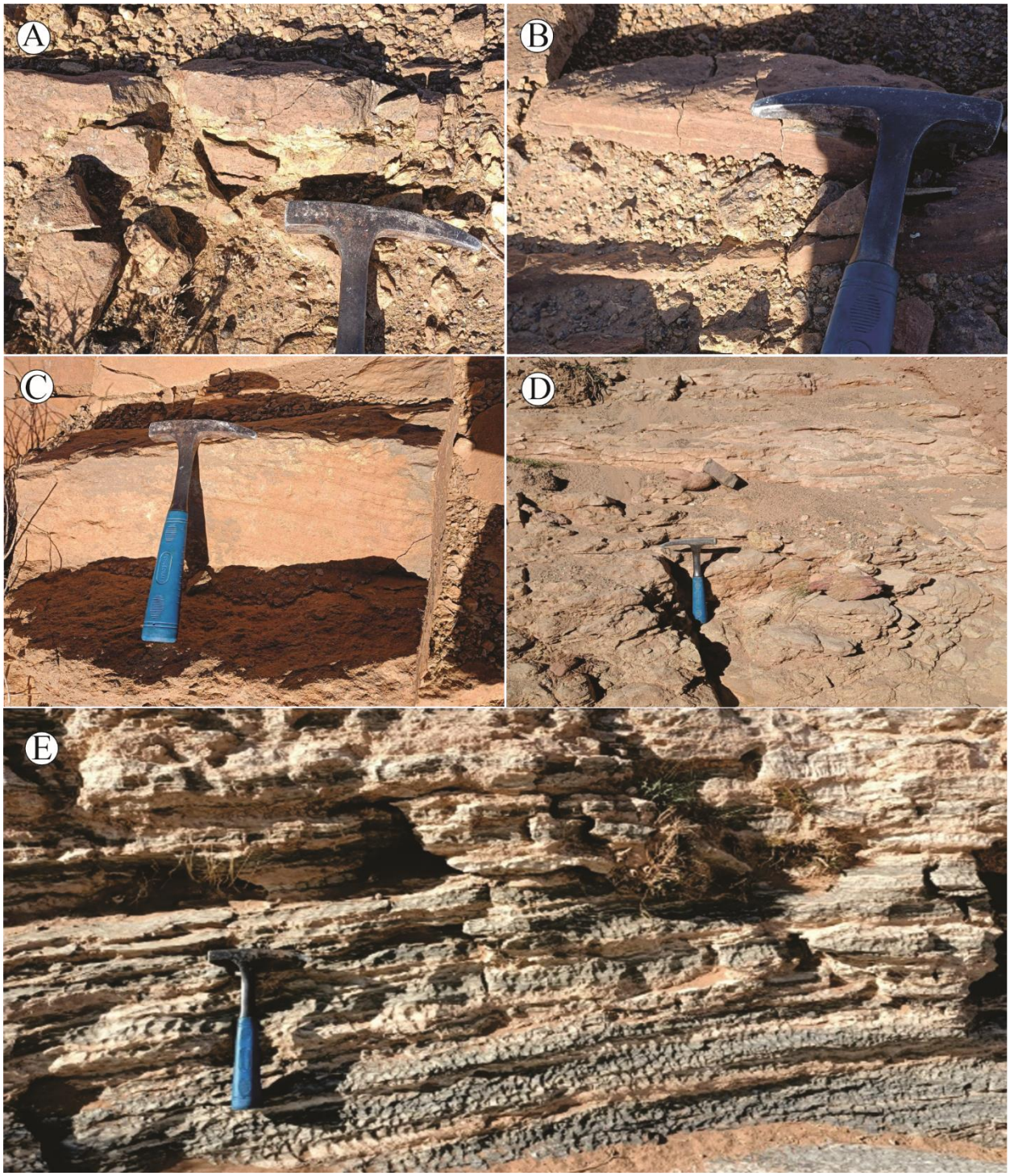


Fig.13: (A) and **(H)**: Shell beds, member 02 ; **(C):** Oolitic limestone, member 2 ; **(D):** Dolostone bed, member 03 ; **(E)** gypsum layers alterning with marls, member 01.

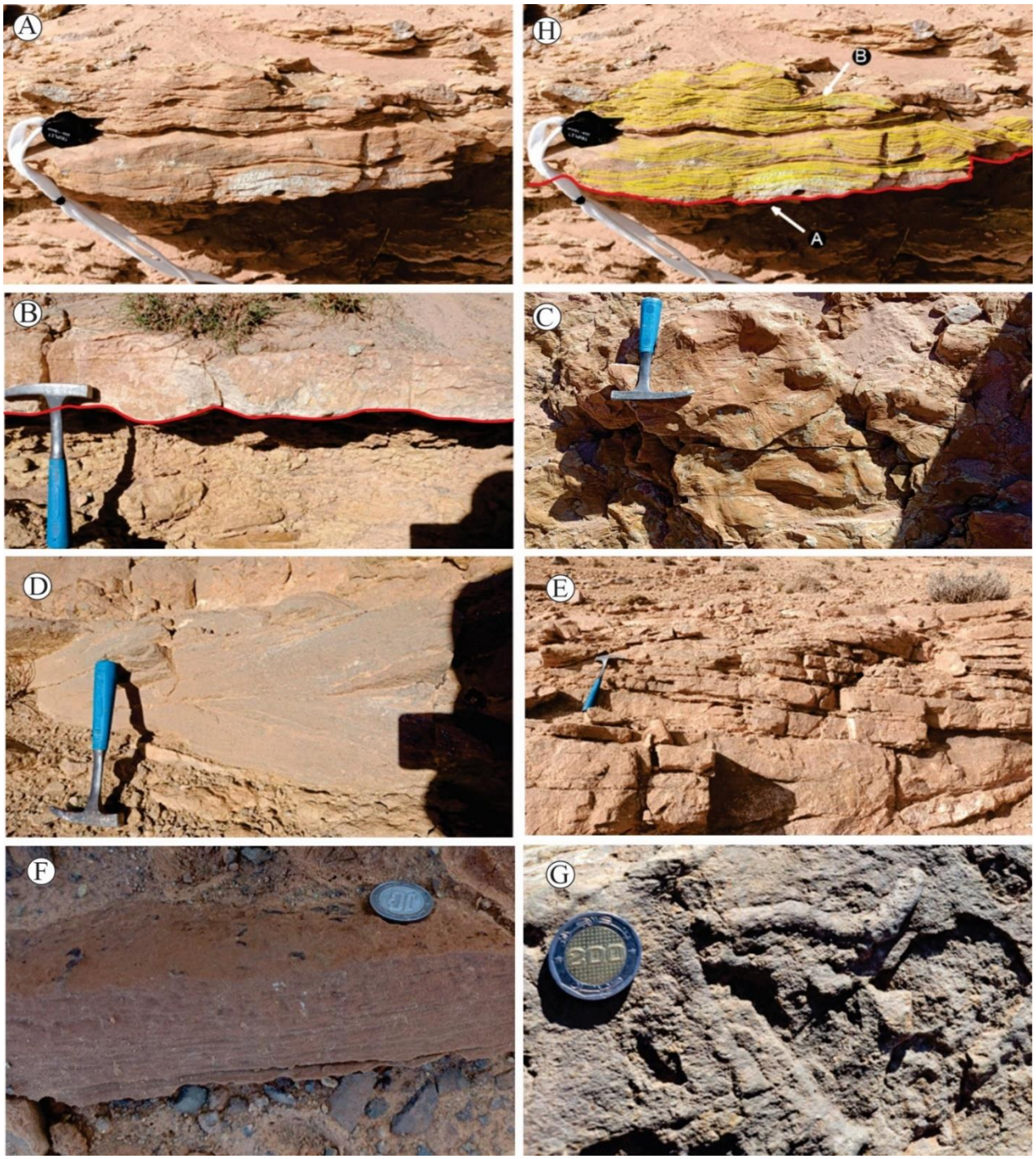


Fig.14: (A) and **(H)**: Hummocky cross stratifications in sandstones showing erosive base (red line in fig H) and with highlighted laminas, member 03, 86m ; **(B):** Erosive base in the dolostones, member 3, 97m ; **(C):** Languid ripples on top of the HCS sandstones, member 03, 86m ; **(D):** Trough cross beddings from the second shell bed of the formation, member 02, 56m ; **(E):** Trough cross beddings from a dolostone bed, member 03, 99m ; **(F):** Parallel laminations, member 02, 62m ; **(G):** Close-up view from the horizontal burrows from the intense bioturbation on the oolitic limestones of the second member, member 03, 88m.

2-Interpretation

Hummocky cross-stratification is a sedimentary structure commonly interpreted as the product of powerful storm waves, due to their frequent association with storm deposits, sediments exhibiting HCS are typically linked to deposition on the continental shelf, HCS in shallow-marine settings is closely linked to wave action and episodic deposition, as evidenced by its occurrence in interbedded sandstones (Collinson and Mountney, 2019). It is generally interpreted as the product of strong and complex wave activity, primarily below fair-weather wave base. The presence of HCS indicates a phase of intense storm-driven sedimentation, followed by lower-energy wave oscillations as conditions calmed. (Collinson and Mountney, 2019). The sharp boundaries between HCS sets indicate erosional surfaces, likely formed by wave scouring or return flows between storm events (Bourgeois, 1980). Such stacking patterns are often interpreted as reflecting rapid sedimentation with little bioturbation, suggesting high storm frequency and limited time for post-storm reworking (Duke, 1985). In many cases, this indicates a proximal storm influence, where wave energy was sufficient to repeatedly rework and deposit sediment without prolonged fair-weather deposition (Myrow and Southard, 1996).

B-Trough cross-bedding

1-Description

Trough cross-bedding is first observed in the shell beds\limestones of the second member, appearing at a centimetric scale (Fig.14D). This structure also occurs in the third member, where it is developed within dolostone beds at a metric scale, reaching thicknesses of up to 1.50 m (Fig,13E). In both limestone and dolostone, sharp boundaries can be observed between the laminae.

2-Interpretation

Trough cross-bedding, which typically indicates a unidirectional depositional process, is associated with the lateral migration of sedimentary structures such as ripples, mega-ripples, or dunes **(**Collinson and Mountney, 2019**).** In wave dominated environments storm-induced currents can generate large scale trough cross-beddings in shoreface deposits (Reineck and Singh 1980).

C- Parallel laminations

1-Description

Some limestone beds show centimetric parallel laminations, characterized by thin laterally continuous layers that maintain a uniform thickness (Fig.14F).

2-Interpretation

These laminations form under conditions of high flow velocity and shallow water depth, characteristic of an upper flow regime flatbed, as the flow accelerates, ripples and dunes are obliterated, and turbulence is suppressed (Collinson and Mountney, 2019). The mode of sediment transport in this setting is interpreted as unidirectional flow (Collinson and Mountney, 2019).

D- Languid ripples

1-Description

This type of ripple is observed exclusively on the epirelief of the terrigenous package, where it occurs at a centimetric scale (Fig.14C).

2-Interpretation

The formation of languid ripple surfaces reflects a decreasing depth with an increase in current velocity **(**Fairbridge and Bourgeois, 1978**)**.

E- Bioturbations

1-Description

The surface of the oolitic limestones beds from the third member are heavily bioturbated, characterized solely by numerous horizontal barrows with sizes varying around 10 cm on the surface and 2 mm in diameter (Fig.14G) forming an extensive network of galleries intersecting and overlapping multiple directions. The oolitic limestone show overall an intense bioturbation with the primary structure of the bed is barely visible due to the abundant borrowing. Others types of borrowing are also present in the second member shell beds.

2-Interpretation

Intense horizontal bioturbation typically results from the activity of infaunal organisms that move parallel to bedding planes, producing a network of burrows and disrupting primary sedimentary features (Ekdale et al., 1984). Such bioturbation suggests prolonged colonization by benthic organisms under calm conditions, often in environments with sufficient oxygen and

organic matter to sustain burrowing fauna (Bromley, 1996). It is commonly associated with low-energy settings such as offshore marine environments, lagoonal deposits, or deep-sea conditions, where low sedimentation rates allow organisms to extensively modify the substrate (Buatois and Mángano, 2011). However, their occurrence in oolitic limestones typically associated with high-energy environments suggests episodic agitation followed by post-depositional stability, allowing burrows to develop (MacEachern and Bann, 2008).

D- Erosive base

1-Description

Many beds from different lithologies such as shell beds, sandstones, and oolitic limestones are characterized by an abrupt, well-defined lower boundary that distinctly separates them from the underlying sediments (Fig.14B).

2-Interpretation

Erosive bases are a common sedimentary structure found across various environments under different conditions. However, they share a common characteristic: formation through high-energy processes that remove pre-existing sediments. These processes include turbidity currents in deep-sea settings (Bouma, 1962) and peak flow events in fluvial systems, particularly in braided and meandering rivers (Miall, 1996), among others. In the Sfissfia Formation, erosive bases are specifically associated with storm-influenced deposits. Tempestite beds are typically coarse-grained carbonate deposits, often characterized by an irregular, erosive base, storm waves and currents can scour the underlying substrate, creating sharp basal contacts beneath storm-generated layers (Myrow et al., 1996).

IV-Carbonates rocks classification system

Microfacies is a petrographic subdivision of a sedimentary rocks defined by its microscopic textural, compositional and diagenetic characteristics as observed in thin section and its nonetheless essential when interpreting rock properties and paleoenvironments (Flugel 2010). All the limestone classifications commonly used in facies analyses are based on textural and compositional criteria. The classifications proposed by (Dunham ,1962) and (Folk ,1962) have proved most practical. Modifications suggested by (Embry and Klovan ,1971), (Wright ,1992) and (Strohmenger and Wirsing.,1991) are of help. Naming and classifying reef limestones, nonmarine carbonates as well as recrystallized carbonate rocks call for specific concepts (Flugel 2010). As in

this study, the classification of limestones and shell beds follow the widely used (Dunham ,1962) with the expansion of (Embry and Klovan ,1971) which is based on the relative contribution of grain support and matrix. Dunham's classification includes five textural classes subdivided according to mud-support (mudstone and wackestone) or grain-support (packstone and grainstone). The subdivision of mud-supported rocks is based on the < or > 10% grain bulk boundary. These rock names can be combined with grain type names in various ways: e.g., Ostracod mudstone (mudstone containing < 10 total rock volume % ostracods), e.g., crinoid packstone (packstone containing a high percentage of closely-packed crinoids), e.g., ooid grainstone (grainstone containing predominantly ooids). The terms floatstone and rudstone were proposed for equivalents of wackestones, packstones and grainstones differing from these rock types in their larger mm- to cm-sized grains. Distinguishing floatstone/wackestone and rudstone/grainstone is particularly meaningful for investigating reef limestones and allochthonous limestones. (Flugel.,2010).

V-Microfacies inventory

Carbonates are present as the most dominant sedimentary rock nature in the Sfissifa Formation, where they are often associated with the shell beds occurring all along the formation. The microscopic study of the upper Kimmeridgian-lower Tithonian Sfissifa Formation yielded 4 carbonate microfacies alongside there Nine distinct sub-microfacies. Thin sections reveal in high percentages a composition of fragmented and, rarely, whole shells of bivalves (oysters) and brachiopods, along with echinoderms and occasional gastropods most of the times enveloped in micrite. These bioclasts range in size from 0.5 mm to over 2 mm and more. Benthic foraminifera are present but negligible, while non-skeletal components, such as ooids, cortoides, aggregate grains, and quartz grains, are notably abundant in most samples (Fig.15). The quartz grains and silt ration are different from the base to top. In below a detailed description of the above mentioned microfacies.

Table. 2: A Classification of carbonates rocks (Dunham 1962); **B** : Classification of Embry and Klovan (1972)

CLASSIFICATION OF LIMESTONES (DUNHAM 1962)

A

DEPOSITION TEXTURE RECOGNIZABLE					DEPOSITIONAL TEXTURE NOT RECOGNISABLE
Original components not bound together during deposition				Original components were bound together during deposition as shown by intergrown or lamination contray to gravity, sediment-floored cavities that are roofed over by organic or questionable organic matter and are too large to be interstices	CRYSTALLINE CARBONATE (Subdivide according classification designed to bear on physical texture or diagenesis)
Contains mud (particles of caly and silt size)			Lacks mud and is grain-suppoerted		
Mud supported		Grain-supported			
less the 10% grains	more than 10% grains				
MUSTONE	WACKESTONE	PACKSTONE	GRAINSTONE	BOUNDSTONE	

EXPANDED CLASSIFICATION (EMBRY AND KLOVAN 1971)

B

ALLOCHTHONOUS LIMESTONE ORIGINAL COMPONENTS NOT ORGANICALLY ORIGINAL BOUND DURING DEPOSITION						AUTOCHTHONOUS LIMESTONE COMPONENTS ORGANICALLY BOUND DURING DEPOSITION		
Less than 10% > 2mm components contains lime mud (<0.03mm)			no lime mud	Greater than 10% > 2mm components		by organisms which		
Mud supported		Grain-supported		Matrix-supported	> 2 mm component supported	build a rigid framework	encrust and bind	act as bafflers
less than 10% grains (>0.03 mm and < 2 mm	geatter than 10% grains					BOUNDSTONE		
MUDSTONE	WACKESTONE	PACKSTONE	GRAINSTONE	FLOSTSTONE	RUDSTONE	FRAMESTONE	BINDSTONE	BAFFLESTONE

1-sub-microfacies: Ooids-Bivalves Rudstone (Rob)

a-description

This texture is composed primarily of concentric (tangential) ooids and disarticulated oyster shells, with samples of the third member showing more articulated shells all embedded within a micrite dominated matrix (Fig.16A). The ooids display varying degrees of micritization with some showing partial infilling of their internal structures by micrite (Fig.16B). Their concentric layers are often obscured or completely replaced by fine grained carbonates (micrite); their sizes are relatively homogenous varying between 0.2mm to 0.5mm only few shows irregular or slightly deformed shapes.

The >2mm oysters shells are dispersed all over the section. Almost all shells are coated by a thin micritic envelope the original shell structure is still partially visible in some fragments, while others appear more altered. The cement is predominantly micritic with a minor presence of sparite. The overall texture is grain supported with micrite acting as the primary binding agent.

b-Interpretation

Rudstone composed of ooids and oysters suggests high hydrodynamic activity. According to (Embry and Klovan ,1971), rudstone consists of coarse-grained, grain-supported carbonates where grains exceed 2 mm in size. This texture indicates high depositional energy, that prevents finer grains from accumulating followed by calmness which is justified by the micritization and the micrite envelopment of bioclasts that was deposited by strong hydrodynamism. The strong presence of concentric ooids reflects very shallow, warm, low-latitude seas, typical of high-energy settings (Flugel ,2010). The fragmentation of oyster shells suggests reworking by waves or storms, consistent with storm-influenced shoals (Kidwell and Holland, 1991).

2-sub-microfacies: Bivalves Floatstone (Fb)

a-description

The Fb texture reveals a matrix-supported fabric dominance of micrite and low presence of sparite, disarticulated oyster shells, ranging in size from 1 mm to 3 mm, are scattered or floating in a fine-grained background (Fig.16C). It is also noticeable there is a low presence of echinoderms.

b-Interpretation

The matrix-supported floatstone and the dominance of micrite, along with the presence of oysters, were most likely formed in a low to moderate-energy marine setting. bioclasts floating in a fine-grained matrix are interpreted to be deposited between the fair-weather and the storm wave bases, by the settling of lime muds in conditions of very low energy (Kidwell et al., 1986) **.** Therefore, the suggested depositional environment is a lagoon or restricted shelf **(**Flugel ,2010).

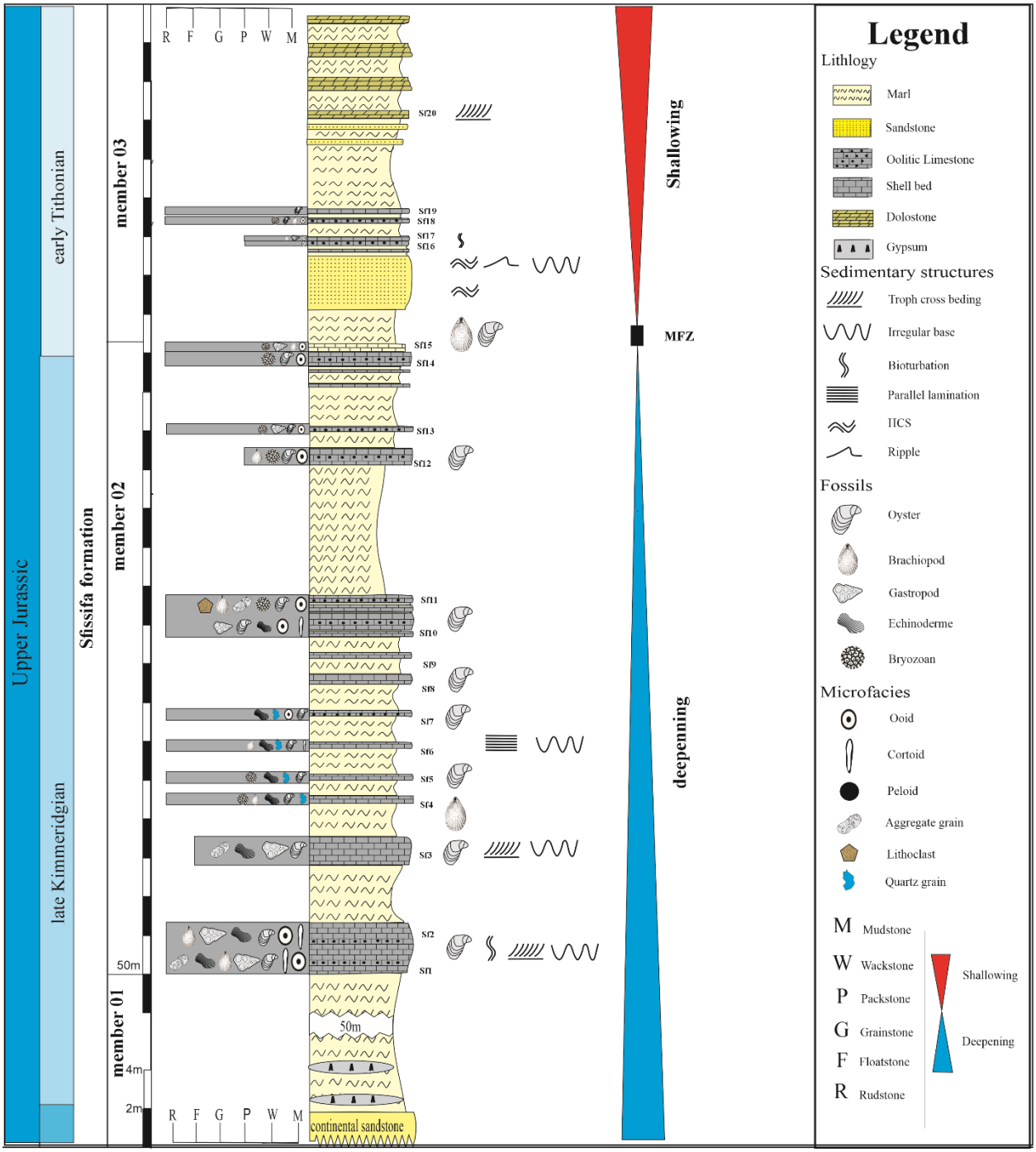


Fig.15: Lithostratigraphic section of Sfissifa Formation.

displaying microfacies data (Sf1-Sf20 samples).

3-sub-microfacies: Bivalves-quartz Floatstone (Fbq)

a-description

Another floatstone was identified, characterized by a matrix-supported fabric dominated by micrite as the cement (Fig.16D), with floating disarticulated and fragmented oyster shells typically around 2 mm in size. However, what differentiates this texture from the previous floatstone is the influence of terrigenous material, as evidenced by the presence of quartz grains.

b-Interpretation

The floatstone texture reflects a low energy environment (Dunham., 1962) and low reworking with previous energetic episode, followed by waning flows with settling of bioclasts and lime muds. This interpretation is further supported by the presence of scattered angular quartz grains that points to the contribution of waning currents that originated in shallower settings (Remírez et al., 2022).

4-sub-microfacies: Bivalves-quartz Rudstone (Rbq)

a-description

This texture exhibits a grain-supported fabric classified as a rudstone. The framework is predominantly composed of bivalve shells larger than 2 mm, occur as fragmented and can be encountered as articulated shells in same cases mostly in the third member. The second most notable feature is the significant influence of terrigenous material (Fig.16E). As mentioned in Fbq, quartz grains are present in varying percentages across different samples (Fig.16F). Additionally, other bioclasts, such as echinoderm fragments and, more rarely, gastropods, are also observed. All these components are embedded within a micrite-dominated matrix. Remark: some samples will show the same texture in addition of a few partially micritized concentric ooids (Fig.16G).

b-Interpretation

Noticeable shell fragmentation and accumulation, a characteristic feature of storm-influenced shell beds and wave reworking (Kidwell and Holland ,1991). The influx of quartz suggests proximity to a nearshore environment, such as a coastal sand shoal (Tucker and Wright ,1990).

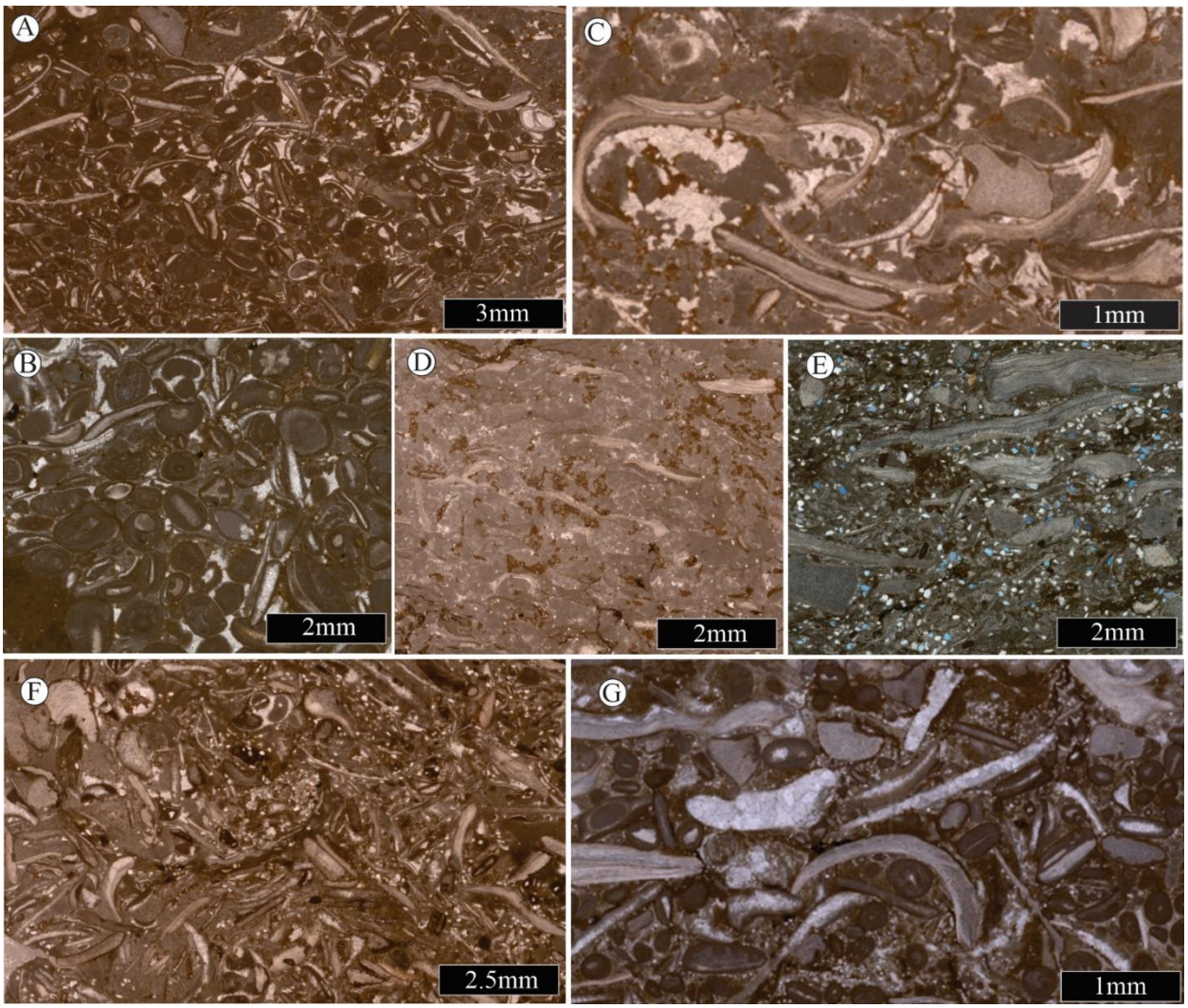


Fig.16: Microphotographs of the main characteristic microfacies of the Sfissifa Formation**. A:** (member 02,sample Sf 1, 50m) Rudstone composed of closely packed bivalve shells (> 2 mm), accompanied by concentric ooids exhibiting partial to complete micritization, all set within a micritic matrix; **B:** a closer look at **A; C:** (member 02,sample Sf 1, 50m) Floatstone displaying scattered bivalve shells >2mm in a micritic dominated matrix; **D:**(member 02, sample Sf 3, 56m) Floatstone composed of bivalve shells scattered in a micritic matrix; **E**:(member02,sample Sf 4, 59m) Show a rudstone composed of bivalves, with abundant quartz grains and a few echinoderm fragments embedded in a micrite matrix; **F:**(member 02, sample Sf 6, 62m) Same texture as D however with a lesser abundance of quartz grains; **G:**(member 02, sample Sf 8, 68m) Same texture as **F** associated with ooids**.**

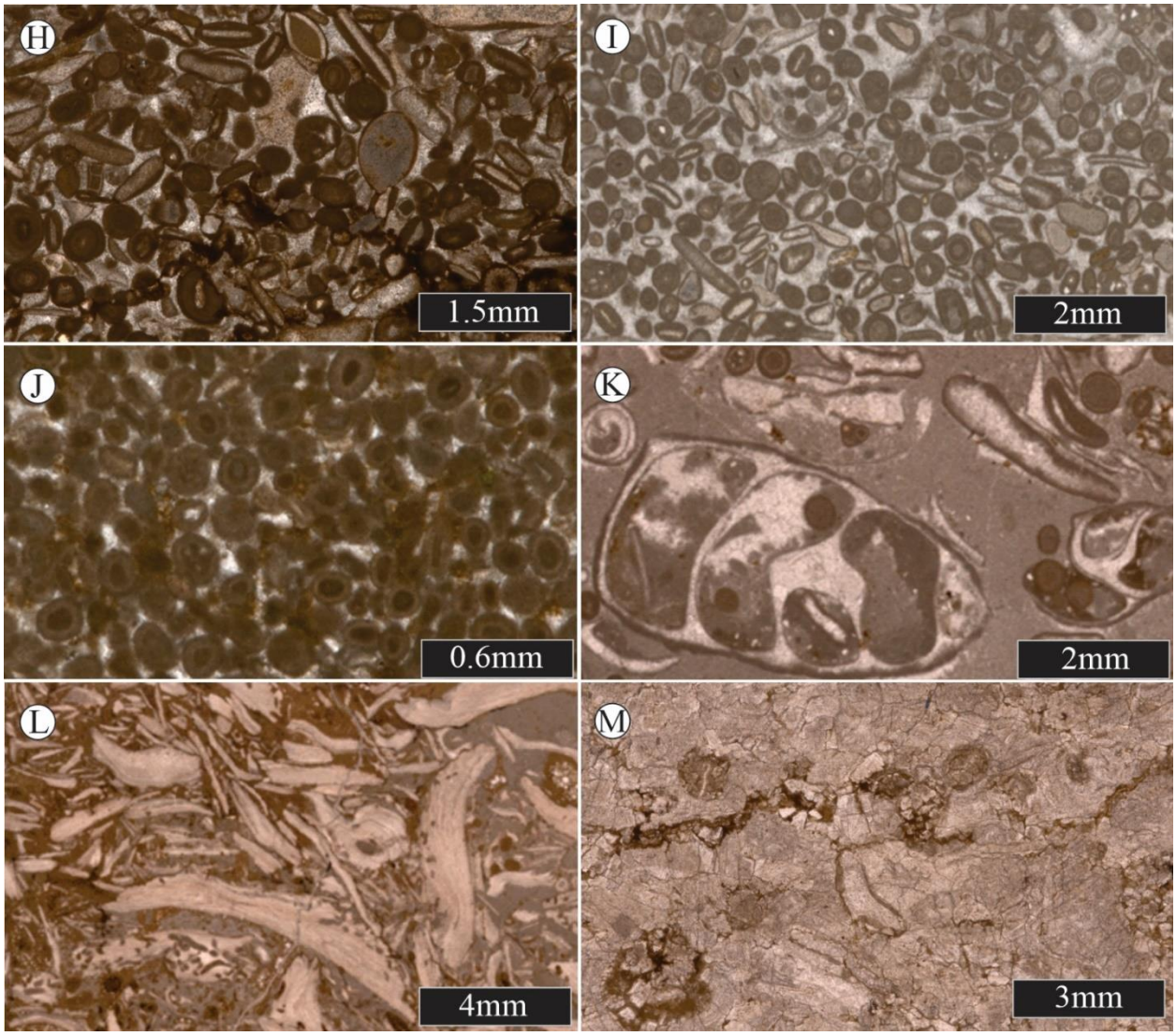


Fig.17 : Microphotographs of the main characteristic microfacies of the Sfissifa Formation **H:**(member 02, sample Sf 10, 70m) Packstone primarily composed of micritized concentric ooids, associated with bioclasts smaller than 2 mm, all enveloped in a micritic matrix ; **I:**(member 02, sample Sf 11, 71m) Grainstone composed of the same components as E, but with a matrix dominated by sparite ; **J:**(member 03, sample Sf 16, 89m) Packstone made only of micritized ooids closely packed in a micrite dominated matrix ; **K:**(member 03, sample Sf 17, 90m) Floastone containing gastropods >2mm scattered along side bivalve fragments in micrite ; **L**:(member 03, sample Sf 19, 91m) Rudstone composed of closely packed fragmented bivalves within a micritic matrix ; **M:**(member 03, sample Sf 20, 96m) Dolostone unclear structures that show possible partial dolomitization of shells.

The presence of ooids in a same sample indicate a deposition in a slightly more energetic setting. These parameters point to deposition by episodic high-energy events, such as storms, between the fair-weather and storm wave-base (Muniz and Bosence, 2018).

5-sub-microfacies: Ooids-bivalves Packstone (Pob)

a-description

A grain-supported packstone primarily composed of concentric ooids and relatively small articulated oyster shells inferior to 2mm with low presence of fragmentation, tightly packed within a micrite dominated matrix with a subordinate presence of sparite (Fig.17H). Most ooids exhibit partial to complete micritization, as described in Rob, and represent the most abundant allochem in the texture. The fragmented bivalve shells, typically smaller than 2 mm, are consistently enveloped by a micritic coating. Additionally, echinoderm fragments are present within the texture.

b-Interpretation

The micritized ooids and shells enveloped in micrite indicate periods of low energy following episodes of agitation, allowing fine carbonate mud to accumulate and coated grains are often are interpreted as indicators of shallow marine warmwater environments (Leonard et al. ,1981**)**. The predominance of micrite suggests a post deposition low-energy environment, such as a lagoon, where micrite precipitation is possible, while the presence of sparite can be explained by an early cementation (Scholle and Ulmer, 2003). Similar facies have been documented in lagoonal and backshoal settings (Tucker and Wright, 1990).

6-sub-microfacies: Ooids-bivalves Grainstone (Gob)

a-description

This texture displays a grain-supported grainstone (Fig.17I) composed primarily of ooids, which exhibit partial micritization, resulting in a less distinct concentric structure. Additionally, oyster fragments, mostly smaller than 2 mm, are present and often enveloped in micrite. Echinoderm fragments are also observed; all embedded within a dominatly sparitic matrix.

b-Interpretation

The presence of concentric ooids indicates high-energy or current-dominated settings with continuous grain movement (Tucker and Wright, 1990). In contrast, the micritization and envelopment of bioclasts in micrite suggest periods of reduced energy conditions, allowing the deposition of fine carbonates a common feature in lagoonal settings or low-energy back-shoal environments (Flugel, 2010).

7-sub-microfacies: Ooids-peloid Packstone (Pop)

a-description

This texture shows a regular grain-supported packstone (Fig.17J), predominantly composed of concentric ooids that exhibit partial to complete micritization. A small percentage of peloids is also present, scattered within a matrix of mixed micrite and sparite, with sparite being relatively abundant.

b-Interpretation

Micritized ooids indicate prolonged exposure in a low-energy setting (Flugel ,2010). This process often occurs in environments with limited agitation, such as lagoons or the deeper parts of shoals (Tucker and Wright ,1990). Peloids typically form in calm settings, possibly within a backshoal or inner ramp (Scholle and Ulmer ,2003).

8-sub-microfacies: Gastropods-bivalve Floatstone (Fgb)

a-description

The framework of this texture is matrix-supported, primarily composed of gastropod (Fig.17K) shells larger than 2 mm, along with disarticulated oysters, noting that all shells are enveloped in micrite. Ooids are also present in small percentages, scattered within a micrite dominant matrix.

b-Interpretation

Bioclasts floating in the matrix are interpreted as having been deposited between the fair-weather and storm wave bases through the settling of lime mud in a very low-energy environment with short time reworking witnessed by the articulated shells (Remírez et al., 2022). They were

then deposited in a low-energy setting with calm waters (Dunham, 1962), such as a lagoon or a protected platform interior, where wave action was insufficient to winnow out fine sediments (Scholle and Ulmer, 2003).

9-sub-microfacies: Bivalve Rudstone (Rb)

a-description

This texture exhibits a grain-supported rudstone (Fig.17L) composed entirely of disarticulated and fragmented bivalve shells larger than 2 mm relatively larger to the previous samples, with a high degree of fragmentation, closely packed within a micritic matrix.

2-Interpretation

The high degree of fragmentation in oyster shells and their dense packing indicate significant physical reworking and winnowing of finer sediments. This is characteristic of tempestites in high-energy shoals, where strong currents or waves remove fine grains **(**Kidwell et al., 1986**)**.

VI- Discussion

Through a sedimentological study and microscopic analyses, it was possible to distinguish various facies and sedimentary structures, along with nine sub-microfacies exhibiting different degrees of packing and composition and some show partial to full dolomitization (Fig.17M). Each sub-microfacies reflects specific depositional conditions. The Sfissifa Formation is primarily composed of carbonate-dominant deposits. The logged section reveals two depositional trends corresponding to transgressive-regressive cycles. The sequence begins with a deepening phase, marked at its base by laminated and lens-shaped gypsum layers overlying the Boualem Formation. These are followed by a thick package of marls, succeeded by alternating shell beds, oolitic limestones, and silty marls. Microscopic analysis of the shell beds and (**L.ts**) from Member 02 identified multiple microfacies, with rudstone and its subfacies (**Rob, Rbq**) being the most common. These subfacies are characterized by an abundance of fragmented oyster shells and other bioclasts (brachiopods, gastropods, etc.), often embedded in micrite and associated with micritized ooids within a micrite-dominated matrix. Another notable feature is the varying abundance of quartz grains, which progressively decrease. The articulated are can be encoutred in this texture

from the samples of the third member Additionally, floatstone textures are present in the first member, represented by two sub-microfacies (**Fb, Fbq**), where disarticulated oyster shells float within a micrite matrix, occasionally accompanied by quartz grains. Member 03 in which the shallowing phase start is characterized by the deposition of the first terrigenous subfacies (**S.hcs**) and (**S.lr**), overlain by oolitic limestones (**L.b**), which contain two packstone sub-microfacies (**Pob, Pop**). The first sub-microfacies (**Pob**) consists of tightly packed micritized ooids with some bivalve fragments, whereas the second (**Pop**) contains micritized ooids along with peloids. Rudstone textures (**Rob, Rb**) are also present, marking the last shell beds of the formation. Finally, followed by the presence of trough cross-bedded dolostone interbedded with marls.

The collected and analyzed data suggest that the Sfissifa Formation was deposited in a nearshore marine environment that was initially relatively calm but frequently disrupted by episodic intense storms. These high-energy events played a crucial role in sediment reworking, leading to the formation of storm-winnowed shell beds and other storm deposits (e.g., Banjamin F. Dattilo and al., 2008). The presence of evaporitic deposits at the base of the formation indicates a shallow coastal environment with periodic evaporation, as evidenced by laminated gypsum associated with fair-weather deposits (marls) as the most abundant facies (e.g. Flügel 2010). This is followed by a succession of shell beds and oolitic limestone, both of which contain abundant fragmented shells, often enveloped in micrite, as well as micritized ooids. These features indicate deposition under episodic intense storm conditions, with varying degrees of winnowing, typical of storm-influenced shoals. The presence of fragmented bivalves and echinoderms further supports episodic reworking due to high-energy events such as storms, followed by periods of post-depositional stability witnessed by the abundance of the micritic matrix and micritization. Other storm deposits, such as (**S.hcs**), further reinforce this interpretation. Altogether, these characteristics suggest that the Sfissifa Formation was deposited in a originally calm shallow marine environment influenced by episodic storm activity, likely in an open lagoon setting connected to the open sea.

Table. 3: Full and summarized inventory of the facies and sedimentary structures with their interpretations

cies	Sub-facies	Abbreviation	Description	Interpretation
bed		SH	Massive shell-rich beds, mostly brown in color, with thicknesses reaching up to 50 cm. They exhibit sedimentary structures such as erosive bases and trough cross-bedding, along with macrofossils, primarily oysters.	Shell beds indicate high-energy deposi events, likely storm-related or wave-influe in a shallow marine setting.
ic tone	Trough cross-bedding oolitic limestone	L.ts	Limestone beds with thicknesses ranging from a few tens of centimeters to 30 cm, brownish in color, often associated with shell beds. They display abundant trough cross-bedding structures.	Oolitic limestone with trough cross-be suggests high-energy shoal or tidal ch deposition, driven by strong currents and fre sediment reworking.
	Bioturbated limestone	L.b	Thinner limestone beds, around 15 cm thick, grey and white in color, characterized by intense bioturbation (horizontal burrows) on the epirelief, with no visible macrofossils.	Indicate formation under episodic intense agitated conditions, followed by a depositional stability.
	Parallel lamination oolitic limestone	L.pl	limestone beds show centimetric parallel laminations, characterized by thin laterally continuous layers that maintain a uniform thickness.	High flow velocity and shallow water dep mode of sediment transport in this setti interpreted as unidirectional flow
stone		Do	massive dolostone beds (15 cm–1 m), yellow on fresh and weathered surfaces, with sharp, irregular contacts over marls and abundant trough cross-bedding.	The dolostone formed through post-deposi dolomitization, altering the original limes driven by Mg-rich brines in arid coastal sett
stone	HCS sandstone	S.hcs	Thickening-upward unfossiliferous sandstone layers (5–20 cm), yellow in color, display abundant vertically stacked hummocky cross-stratification (HCS).	Indicates storm-dominated deposition in a shoreface to offshore transition zone, form oscillatory and combined-flow currents d storm events.
	Languid ripples sandstone	S.lr	20 cm sandstone layers overlying the HCS structures are characterized by languid ripples	The formation of languid ripple surfaces re a decreasing depth with an increase in cu velocity.
		Mr.	From few centimeters to 8m deposits of carbonate-rich marls with silty siliciclastic input, predominantly brown, and mostly unfossiliferous, except for two brachiopod-rich levels. The second level transitions to a greenish color.	Indicate a low-energy depositional environ where sediments accumulated under rela calm conditions with limited hydrodyn influence.
ım		Gy	gypsum occurs in two forms, centimetric parallel layers alternating with marls and lenticular bodies, either isolated or as thin, discontinuous layers within the marls, with centimetric size	suggests deposition in a restricted, evap environment, such as a coastal sabkha or s where there is high evaporation

Table. 4: Full and summarized inventory of the microfacies data and their energetic interpretations

Rudstone	Ooids-Bivalves Rudstone	(Rob)	Consists of concentric ooids (0.2–0.5 mm) and disarticulated oyster shells (>2 mm). Ooids show micritization, some with partial infilling, while oyster shells are scattered, coated with micrite, and variably preserved. Cement is mostly micrite with minor sparite, and the texture is grain-supported.	indicates high-energy shoal or proximal platform environments, where strong currents facilitated ooid formation, shell accumulation.
	Bivalves-quartz Rudstone	(Rbq)	A grain-supported, mainly composed of fragmented bivalve shells (>2 mm) with varying quartz content and minor echinoderm and gastropod fragments. Micrite matrix, with some samples also containing partially micritized ooids.	likely a nearshore and storm-influenced environment where wave and current action concentrated shell debris and quartz grains.
	Bivalve Rudstone	(Rb)	This grain-supported rudstone consists entirely of articulated and fragmented bivalve shells (>2 mm) tightly packed within a micritic matrix.	indicates a high-energy, storm-influenced or wave-dominated setting, where rapid deposition and limited transport preserved dense shell accumulations.
Floatstone	Bivalves Floatstone	(Fb)	matrix-supported texture , dominated by micrite with minimal sparite. Fragmented oyster shells (1–3 mm) are scattered in a fine-grained background, with a low presence of echinoderms.	low- to moderate-energy marine setting, where shells were deposited with little transport.
	Bivalves-quartz Floatstone	(Fbq)	matrix-supported with micrite cement, containing floating fragmented oyster shells (~2 mm). Characterized by its terrigenous influence, shown by scattered quartz grains.	low to moderate energy conditions with siliciclastic influx from nearby land sources while still maintaining a carbonate-dominated environment.
	Gastropods-bivalve Floatstone	(Fgb)	This matrix-supported texture consists mainly of gastropod shells (>2 mm) and fragmented bivalves, all coated in micrite. Scattered ooids are present within the micrite-dominated matrix.	low- to moderate-energy marine setting
Grainstone	Ooids-bivalves Grainstone	(Gob)	Consists mainly of partially micritized ooids, with less distinct concentric structures. It contains oyster fragments (<2 mm) coated in micrite, echinoderm fragments, and a predominantly sparitic matrix	deposition in a high-energy, shallow marine environment suggesting strong hydrodynamic conditions with continuous reworking
Packstone	Ooids-bivalves Packstone (Pob)	(Pob)	Dominated by micritized ooids and fragmented oyster shells (<2 mm) in a micrite matrix with minor sparite, along with echinoderm fragments.	moderate-energy deposition in a shallow marine setting, with periodic reworking allowing ooid and shell accumulation within a micritic matrix.
	Ooids-peloid Packstone (Pop)	(Pop)	This grain-supported packstone consists mainly of micritized concentric ooids, with scattered peloids in a mixed micrite-sparite matrix, where sparite is relatively abundant.	moderate-energy deposition in a shallow marine setting, likely a lagoon or protected shoal, where ooids and peloids accumulated.

Table. 5: samples taken exact locations in the Sfissifa form

Sample Number	Member	high
Sf1	Member 1	50m
Sf2	Member 1	53m
Sf3	Member 1	56m
Sf4	Member 1	58.5m
Sf5	Member 1	60m
Sf6	Member 1	62m
Sf7	Member 1	64m
SF	Member 1	65m
Sf9	Member 1	67m
Sf10	Member 1	68m
Sf11	Member 1	70m
Sf12	Member 1	76m
Sf13	Member 1	78m
Sf14	Member 1	81m
Sf15	Member 1	82m
Sf16	Member 2	87.5m
Sf17	Member 2	88m
Sf18	Member 2	88.5m
Sf19	Member 2	89m
Sf20	Member 3	94m

Chapter four

Shell beds

I -Introduction

This chapter deals with the taphonomy and the genesis of the shell beds within the Sfissifa Formation, but first a brief introduction and definitions about shell beds and their mode of formation base on a synthesis done by (Fürsich, F., 1995) followed by an overview of shells concentrations classification.

I.a-How do shells concentrations form?

Three majors factors control the formation of shell concentrations (Fig.18): (1) biological processes, (2) physico-chemical processes and (3) time.

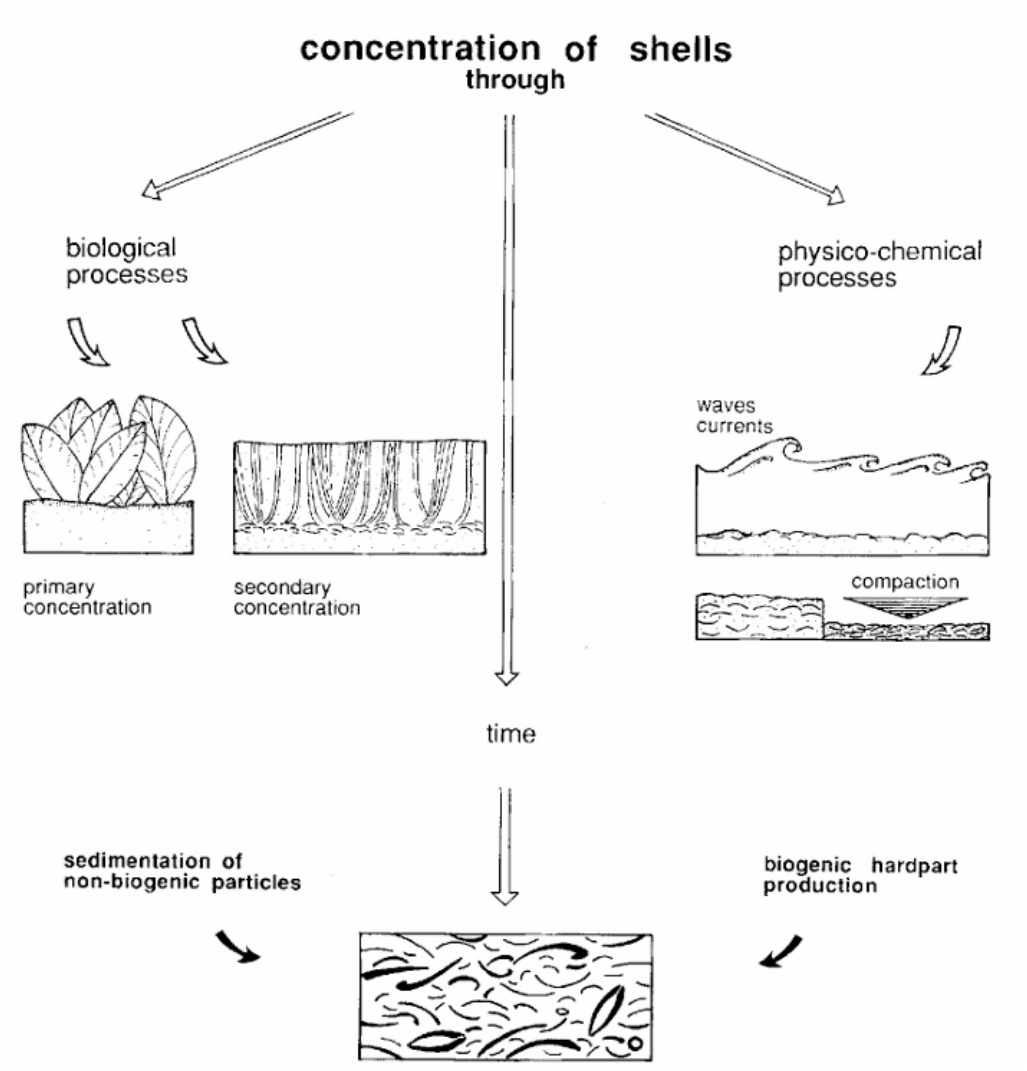


Fig.18: The key factors controlling shell concentration formation (Franz., 1995).

Physical processes are the most important agents for the concentration of biogenic hard remains. Whereas, chemical processes, more or less restricted to compaction (diagenetic processes), play a minor role. Among the key physical agents: waves, currents, and turbidity flows. These mechanisms contribute to the concentration of skeletal remains either through the removal of finer sediments (winnowing) or by selectively transporting certain components (Franz., 1995). Many examples illustrate this, such as shell pavements at the base of tidal channels, storm-generated shell beds as in our studied case, and shell bars (Rodriguez.,2022), (Rodriguez.,2024).

Shell concentrations may, sometimes, result from the activities of the constituent organisms themselves.

This can happen through various biological behaviors processes like gregarious settling which may associated with opportunistic life strategies. Another significant mechanism is mass mortality event, which may be triggered by a range of biotic or abiotic stressing factors such as harmful algal blooms, abrupt shifts in water chemistry, temperature, or rapid sedimentation episodes. These events generally reflect a biological response to sudden environmental perturbations. Alternatively, shell concentrations can be triggered organisms that actively gather the remains of other species. These concentrations often result from specific feeding habits, such as the shell pockets created by rays (Gregory et al., 1979), or the shell-rich deposits produced by the burrowing activities of the lugworm *Arenicola marina* (Van Straaten, 1952). Additional behaviors mechanism includes the use shells for burrow backfilling or wall constructions, can also lead to localized shell accumulations.

Time plays a crucial role in the development of shell concentrations, either directly by influencing the duration of accumulation or indirectly, through sedimentation rates of non-biogenic material and the production of skeletal remains. Even when biogenic production is low, slow net sedimentation can still lead to the formation of condensed shell deposits. Often, several factors interact in the formation of these shell concentrations, which makes identifying their origins and history particularly a challenging task (Franz., 1995).

I.b-Descriptive classification of shell beds

Descriptive classification of shell concentrations provides a variety of ecological, hydrodynamic, and topographic insights (Kidwell et al. 1986). This approach takes into account

three key attributes (1) taxonomic composition, (2) bio-fabric, (3) geometric arrangement of the shell concentration (Fig.19). The taxonomic composition reflects the original biological communities offering insight about palaeoecological conditions. However, this ecological signal is often altered by taphonomic processes, such as hydraulic sorting of shells based on their size or shape. These processes, in turn, reflect the hydrodynamic environment in which the deposit formed. Based on this information, we can classify shell concentrations as monospecific, paucispecific, or polyspecific, following the framework proposed by (Kidwell et al. 1986).

The three-dimensional arrangement of skeletal elements reveals the hydrodynamic conditions during deposition, with secondary influence of compaction and ecological aspects.

biofabric characteristics including shell orientation, packing density, and how well they are sorted, can provide critical clues into depositional environment, the original topography of the area, and sometimes point to the agents responsible for the accumulation, whether they were living organisms, waves, or currents. the internal architecture of shell concentrations such as: their composition, structure, and matrix change both laterally and vertically provides insight into its formation history. This includes whether they formed from a single event or multiple ones, while also providing temporal constraints on their formation.

I.c-Genetic classification of shell beds

Shell concentration is considered to be important for their potential as environmental indicators. (Fürsich and Oschmann., 1993) developed a classification scheme applicable to epicontinental seas in general. Nine genetic types of shell concentrations, related to the relative importance of the main concentration processes (waves, currents, biological productivity, biological activity, net sedimentation, and time), can be distinguished. These types exhibit distinct bathymetric trends and thus serve as excellent tools in basin analysis.

Fair-weather wave concentrations

These deposits are continually shaped and modified by wave action, resulting in clear taphonomic signatures such as signs of abrasion, and fragmented shells. Shells are always disarticulated and hydraulically well sorted. When viewed from above, they typically show a bimodal orientation pattern.

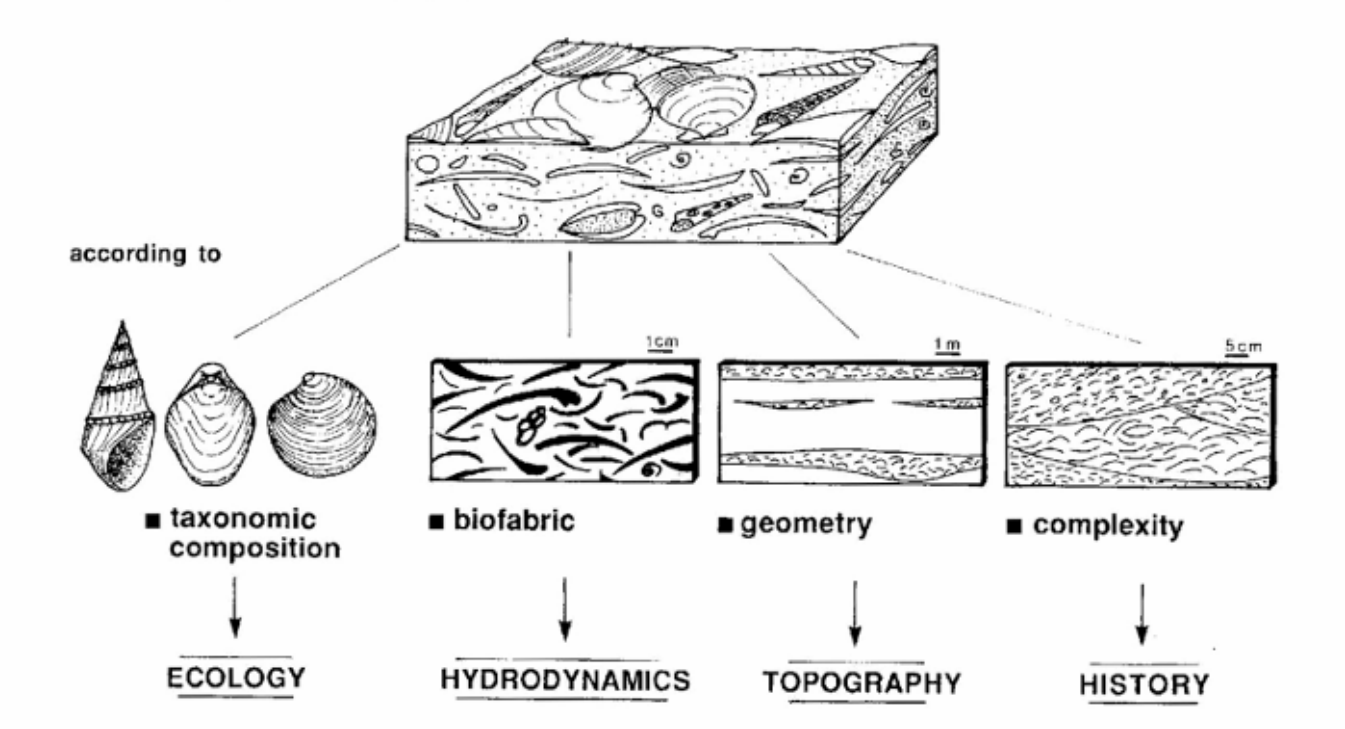


Fig.19: the descriptive classification of shells concentrations (Franz., 1995)

Storm wave concentrations

These deposits are better preserved since reworking happens over a short time. If a living community is disturbed, many shells may remain articulated. Sorting is usually minimal, and infaunal shells tend to show no signs of boring or encrustation.

Proximal tempestites

These deposits share several features with storm wave deposits but also show clear signs of transport. The shells are generally in good condition (relatively well-preserved), and the deposits often have a sharp, erosive base with normal grading. The shells are often disarticulated and lie convex-up.

Distal tempestites

These deposits differ from the proximal ones by thinner beds, bearing smaller skeletal fragments. They are also very well sorted and graded.

Current-driven concentrations

Shell concentrations formed under tidal, longshore, or other shelf currents show variable preservation states. While, convex-up shell orientation and poorly preserved shells are common, depending on how long the shells remained exposed to currents.

Primary biogenic concentrations

They result from the gregarious settling of larvae or from low sedimentation rates. Some shells may be preserved in their life position, and original patterns of colonization, like nests, might be retained.

Winnowed concentrations

They develop as pavements or thin shell layers. They result from selective removal of finer sediments by low-energy currents, while denser sediments and denser bioclasts remain as residual deposits. The retained shells often exhibit exceptional preservation due to minimal hydraulic transport.

Transgressive lag concentrations

They develop over extended time periods, often show multiple phases of reworking and erosion, alongside with low sedimentation rates. These lags typically form during transgressive phases in epicontinental seas, where retreating shorelines expose older deposits to shelf currents and storms. The resulting deposits bear a mixture of shells with prolonged seafloor exposure, poor to moderate preservation, and common signs of bioerosion like boring and encrustation.

Condensed concentrations

These deposits represent the longest time spans on seafloor exposure. They commonly contain bored, encrusted, or corroded shells, with small and delicate forms often absent due to bioerosion or chemical dissolution. Consequently, the result corresponds to an assemblage dominant by thick and robust forms. However, because new material is added periodically integrated over time, some shells may be exceptionally well preserved.

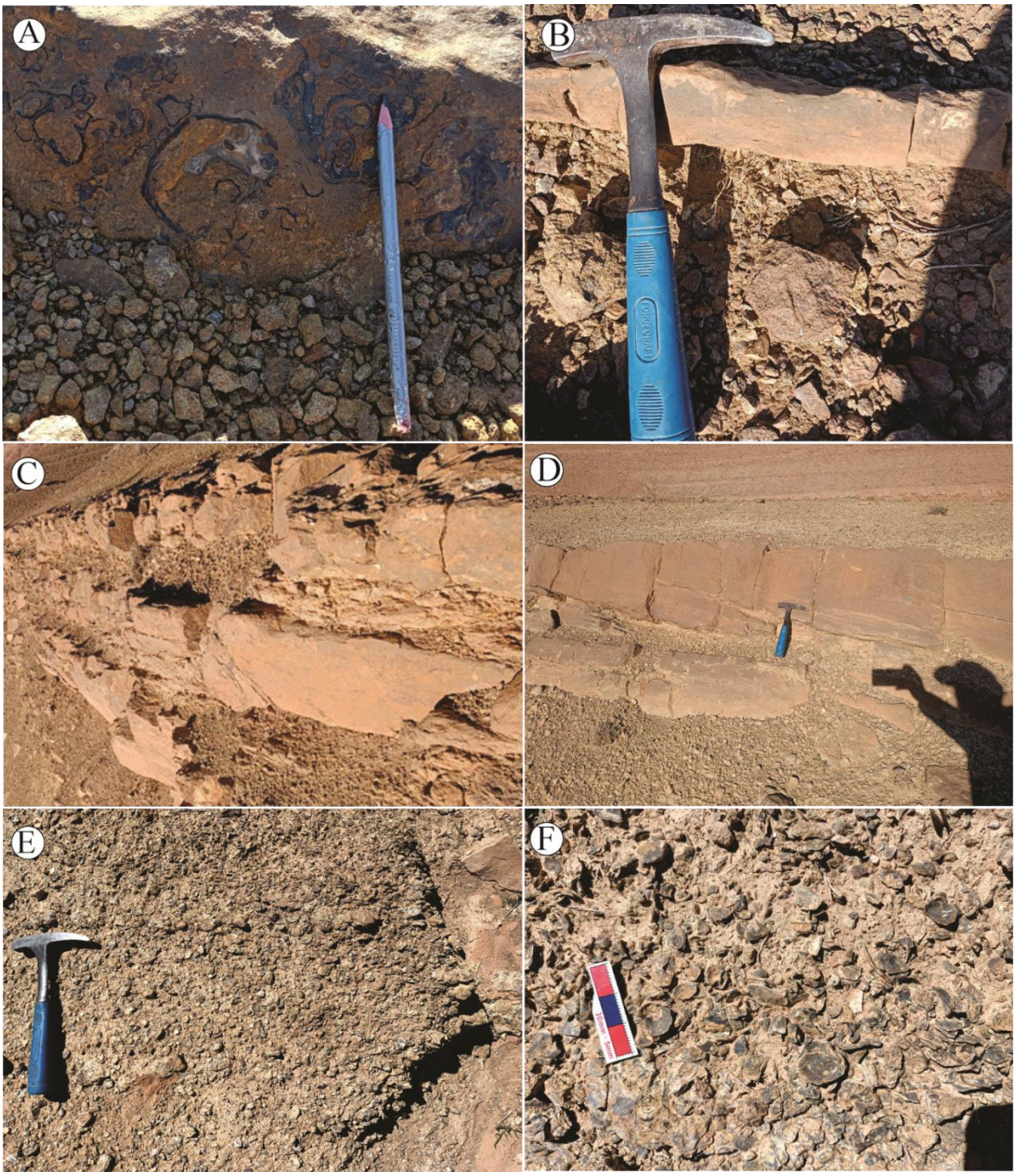


Fig.20: (A): Centimetric disarticulated oysters shells**; (B):** Thin shell bed with visible oysters shell fragments; **(C)\(D)**: Beds of shell beds and oolitc limestone; **(E)**: Plain view of a shell concentration made from oysters shells; **(F)**: close up look at E.

II –Sfissifa Formation shells concentrations

The previously nine described carbonates microfacies in chapter 3 are organized into different carbonates shell beds with irregular contacts, separated by silty marls intervals, which are described below both on a macroscopic and microscopic scale. (see chapter 3 for the description and interpretations of the present microfacies).

(Rob: Ooids-Bivalves Rudstone **– Fb:** Bivalves Floatstone **– Fbq:** Bivalves-quartz Floatstone **– Rbq:** Bivalves-quartz Rudstone **– Pob:** Ooids-bivalves Packstone **– Gob:** Ooids-bivalves Grainstone **– Pop:** Ooids-peloid Packstone **– Fgb:** Gastropods-bivalve Floatstone **– Rb:** Bivalve Rudstone**).**

II.a –Description

The skeletal accumulations in Sfissifa Formation consist of yellowish-brownish carbonates shell beds ranging from 5 cm to nearly 50 cm in thickness displaying shells that can reach centimetric scales (Fig.20A). They can occur in three aspects, massive, continued thin layers and lens-shaped. And can encountered under two types of cementation, well cemented and hard or weak cemented and friable (Fig.20E-F). Nearly all exhibit sharp erosional basal surfaces (Fig.20B), along with sedimentary structures such as trough-cross beddings, as well as bioturbations that will play a major role in organization of the bioclasts.

The accumulations can form continuous shell beds. However, the thickness varies laterally. Some shell beds maintain a uniform thickness (Fig.20C), while others thin and thicken irregularly, forming lenticular shapes (Fig.20D). On a macroscopic scale the skeletal accumulation is predominantly consisted of disarticulated and/or fragmented oysters shells (Fig.20E-F). However, complete articulated shells can be common in some cases (third member), the sizes of the bioclasts can range from a few millimeters to 5 cm maximum. Shell orientation varies between beds. In some beds, the shells are randomly arranged, and influenced by an intense burrowing that led to a rearrangement of the orientation of the shells, and altering their original biofabric. Grading can be often a feature observed in some shell beds, where bioclasts start as small millimetric fragments at the base to bigger even centimetric disarticulated shells.

From a microscopic point of view, nineteen thin sections revealed nine distinct microfacies: **Rob, Fb, Fbq, Rbq, Pob, Gob, Pop, Fgb**, and **Rb**. Rudstone textures are the most common

throughout the Sfissifa Formation. In some shell beds, **Rob** alternates with **Fb** in multiple fining-upward successions. **Rob** is the most abundant texture, and represents the thickest beds, characterized by densely packed, poorly sorted, disarticulated shells along with other fragmented shells. Some large articulated shells relatively in small percentage, all lacking any preferential orientation. The **Fb** microfacies, in contrast, is more loosely packed and contains mostly articulated shells.

Another microfacies dominated entirely by the **Fbq** texture similar to floatstone described above, however with a terrigenous influence. Shell beds from the second member are mostly composed of a single dominant microfacies: **Rbq,** with **Sf4** and **Sf5** where articulated shells are very common with some disarticulated\fragmented shells, mainly obliquely oriented to the bedding intercalated by **Fbq**. These facies are marked by densely packed, disarticulated, and fragmented oyster shells, randomly oriented and disoriented by bioturbation, which likely disrupted their original orientation. These beds also show varying degrees of terrigenous influence.

The cooccurrence of two microfacies **Rob** and **Pob** in several fining-upward successions is common in Sfissifa Formation, with **Rob** being dominant. **Rob** in this bed shows densely packed, disarticulated, and fragmented shells that are poorly sorted and lack a consistent orientation. **Pob,** the secondary microfacies, contains few small-sized shells, highly fragmented, and densely mixed with ooids.

The **Pob** microfacies dominates completely some beds, showing only fragmented shells with varied orientations. Other shell beds display a mixture of **Rb** and **Rob** microfacies. Both show disarticulated and fragmented but articulated ones are common, without clear orientation, likely affected by bioturbation.

The third member is mainly composed of **Pob** interbedded with **Fgb**. The **Fgb** microfacies features loosely packed, poorly sorted shells of gastropods and bivalves, mostly whole or disarticulated, and occasionally fragmented.

II.b –Taphonomic and genetic interpretation of the shell concentration

The shell concentration shows several noticeable features, most importantly the high number of articulated shells found in uppermost of the Sfissifa Formation. Sorting is very poor, and unlike classic storm related shell beds (Fürsich, F. T., 1986), the shells here almost never show

a favorable orientation, random arrangements are quite common. Altogether, these features point to only limited reworking before burial, which point to the fact that the shells were not transported far from where the organisms lived and died.

The concentrations likely formed in place through gregarious settling behavior (such as dense oyster communities or brachiopod aggregations), or as a result of high population densities enabled by particularly favorable environmental conditions, in other words the shells are autochthonous to parautochthonous and were shortly transported from a nearby calm soft fine grained sea floor where they will be influenced by episodic high energetic events likely to be storm followed by stability explained by the redeposition of the fine sediments and the abundance of micritization as shown in the thin sections.

The fragmented shell are also present through the Sfissifa Formation with a decent amount in different condition they would be interpreted as being deposited in a high energy environment, however that contradict what is present, as the marl/silty marl (most abundant facies) clearly represents an environment below the fair-weather wave-base, so the most possible suggestion for the fragmentation is interplay of opportunistic organism (e.g., Buatois, L.A., Mángano, M.G., 2011) that feed on the oysters by breaking through their shells, which is evident in many cases from the clearly reoriented shells and the lack of sorting.

The shell beds of Sfissifa Formation can be classified as monospecific shells concentration due to the lack of faunal diversity, where it was identified *Africogryphaea* shell concentration and The *Pseudexogyra* concentrations (Sadji et al., 2025). This lack of benthic faunal diversity can be associated to two factors.

1) First the hypersaline conditions caused by the gypsum deposits that caused stressed environmental conditions which will limit living conditions.
2) The second factor can be the dissolution of shells made of high percentage of Mg or aragonitic shells while the conserved shells are made of low Mg shells, which will lead to the suggestion of a presence of paucispecific concentrations during early diagenesis (Fürsich and Oschmann., 1986).

In summary, the shell concentrations in the Sfissifa Formation appear to have a mixed origin as explained, resulting from a combination of biogenic, diagenetic, and physical processes that worked together during their formation.

III –Paleoenvironment synthesis

The presence of evaporitic deposits at the base of the Sfissifa Formation indicates deposition in intertidal to supratidal zones, or within shallow, restricted subaqueous environments such as Salinas (Warren and Kendall, 1985; Flügel 2010), consistent with arid to semi-arid climatic conditions. The dominant facies -marl and silty marl- suggest low-energy deposition, likely within a lagoonal system.

Interbedded cross-bedded oolites and sandstones within the Sfissifa Formation point the presence of shoals within this lagoon, shaped by occasional higher-energy conditions. Additionally, the occurrence of sandstone layers, the presence of silts and quartz grain in the carbonates indicate siliciclastic material input from nearby continental sources. Shell beds are present under the form of various origin (biogenic, diagenetic and physical). The Sfissifa Formation displays evidence of episodic high-energy events that interrupted the calm lagoonal settings. All this point to a shallow and proximal position relative to the shoreline.



Conclusion



General conclusion

The Sfissifa Formation is a Late Jurassic unit in El Bayadh region of the central Saharan Atlas (Amour Mountains). Overlying the sandstones of the Boualem Formation, it has been subdivided into three members:

The first member**:** with 1.5 m-thick gypsum-rich interval, followed by yellow to green unfossiliferous marls containing gypsum lenses.

The second member**:** consists of 32 m-thick of alternating bioclastic limestone and marl. The limestone beds are rich in oyster remains, with the base marked by a thick, laterally variable shell bed composed mainly of oysters, brachiopods, and occasional gastropods. Occasional ooilitic limestone are also present.

The third member**:** begins with a second brachiopod-rich marl level, marking the transition into the early Tithonian. This interval is characterized by increased siliciclastic input, with interbedded marl and sandstone showing HCS and ripple marks. The upper part includes dolostone beds and partially dolomitized shell layers, with only sparse macrofossils. The Sfissifa Formation culminates with the Continental Intercalaire.

The Sfissifa Formation was originally ascribed to the late Kimmeridgian. However, based on brachiopods assemblages identified in our study, its age range has been extended into the early Tithonian. Thus, the Sfissifa Formation is now dated to the late Kimmeridgian-early Tithonian.

The Sfissifa Formation yielded specie and genu of oysters new to science; *Africogryphaea geniculata*.

The depositional environment of the Sfissifa Formation has been reconstructed based on it sedimentological features; including macroscopic data (facies, and sedimentary structures) microscopic data. This later, various carbonate textures, such as grainstone, floatstone and rudstone, with abundant shell remains, ooids, and cortoids.

These findings indicate that the Sfissifa Formation was deposited in a of environments, from restricted evaporitic settings (gypsum facies) to a shallow marine environment under influence of occasional storms (e.g., shell beds). The presence of evaporites at the base points to

intertidal to supratidal settings in an arid to semi-arid climate. The predominance of marl and silty marl indicates deposition in a calm, lagoonal setting, while cross-bedded oolites and sandstones suggest temporary shoal development during energetic events. The presence of quartz and silt grains in the carbonates indicates input from nearby continental sources. The succession shows a transgressive trend in the first and second members, followed by a regressive phase starting at the top of the second brachiopod rich level.

Based on macroscopic observations of some weak cemented shell beds (sedimentary structures, taphonomy, bed geometries… etc.), some the shell beds in the Sfissifa Formation suggests limited reworking and minimal transport of oysters shells. Unlike typical storm-related shell beds, these concentrations likely formed close to where the organisms lived and died. The origin is autochthonous to parautochthonous, with occasional short-distance transport during brief storm events. This interpretation is supported by: 1) the presence of fine sediments and 2) the widespread micritization observed in thin sections, and 3) the distribution of some shell fragments, which does not reflect high-energy conditions. The shell beds of the Sfissifa Formation reflect a complex interplay of biological, physical, and early diagenetic processes. The overall depositional environment was shallow and nearshore, with a mix of low-energy conditions and occasional high-energy episodes.

References

Abed, S (1982). Lithostratigraphie et sédimentologie du jurassique moyen et supérieur du Djebel Amour (Atlas saharien central, Algérie). Thèse 3ème cycle, PAU, 242p

Ait Ouali, R. (1991) Le rifting des monts des Ksour au lias. Organisation du bassin, diagénèse des assises carbonatées. Place dans les ouvertures mésozoïque du Maghreb, thèse de Doctorat_és_ sciences, Alger, 297 p, 147 fig.

Aït Ouali, R., Delfaud, J. (1995) Les modalités de l'ouverture du bassin des Ksour au Lias dans le cadre du « rifting » jurassique au Maghreb. *Cahiers de Recherches Académiques Scientifiques de Paris*, série IIa, 320, pp. 773–778.

Almeras, Y., Elmi, S., Mekahli, L., Ouali Mehadji, A., Sadik, D., Tlili, M. (1994) Biostratigraphie des Brachiopodes du Jurassique moyen dans le domaine atlasique (Maroc Algérie). Contraintes environnementales et relation avec l'évolution verticale des peuplements d'ammonites. In: Cresta, S., Pavia, S. (Eds.), Proceedings of 3rd International Meeting on Aalenian and Bajocian Stratigraphy, Marrakech, 25–31 May 1994. Miscellanea 5, Roma 219–241

Bassoullet, J.P. (1973) Contribution à l'étude stratigraphique du Mésozoïque de l'Atlas saharien occidental (Algérie). Thèse de Doctorat ès Sciences Naturelles, Université de Paris VI, 497 p., 50 fig., 32 pl.

Benadla. M., Marok. A., Soulimane. C., Reolid. M. (2023) Ostracods of the Cenomanian-Turonian transition in the Ksour and Amour Mountains (Saharan Atlas, Algeria): systematic and palaeobiogeographic implications.*Estudios Geológicos 79(1):e152*

Benjamin, F. Dattilo., Carlton, E. Brett., Cameron, J. Tsujita., Robert, F., (2008) Sediment supply versus storm winnowing in the development of muddy and shelly interbeds from the Upper Ordovician of the Cincinnati region, USA, Canadian Journal of Earth Sciences 45 (2): 243–265.

Benyoucef.M., Mebarki.F., Ferré.B., Adaci.M. (2017) Litho- and biostratigraphy, facies patterns and depositional sequences of the Cenomanian–Turonian deposits in the Ksour Mountains (Saharan Atlas, Algeria). *Cretaceous Research*, 74, 44–63.Bettahar, N.

Bessedik, M., Mammeri, C., Belkebir, L., Mahboubi, M., Adaci, M., Hebib, H., Bensalah, M., Mansour, B., Mansouri, M.E.H. (2008) Nouvelles données sur les ichnites de dinosaures de la région d'El Bayadh (Crétacé inférieur, Algérie). Palaeovertebrata 36, 7–35.

Boggs, S. (2006) *Principles of Sedimentology and Stratigraphy*, 4th ed. Pearson Prentice Hall, Upper Saddle River, New Jersey, 662 p.

Bouma, A.H. (1962) Sedimentology of Some Flysch Deposits and the "Bouma Sequence". In: Sedimentology by P.H. Kuenen, pp. 345-389.

Bourgeois.J. (1980) A transgressive shelf sequence exhibiting hummocky stratification; the Cape Sebastian Sandstone (Upper Cretaceous), southwestern Oregon, Journal of Sedimentary Research (1980) 50 (3): 681–702.

Bracène R, Frizon de Lamotte D. (2002) Origin of intraplate deformation in the Atlas System of western and central Algeria: from Jurassic Rifting to Cenozoic–Quaternary inversion, Tectonophysics 357 (1–4)

Brett, C.E., Baird, G.C. (1986) Comparative Taphonomy: A Key to Paleoenvironmental Interpretation Based on Fossil Preservation pp. 207-227 (21 pages), SEPM Society for Sedimentary Geology

Bromley, R.G. (1996) *Trace Fossils: Biology and Taphonomy*. 2nd ed., Chapman and Hall, London, 361 p.

Buatois, L.A., Mángano, M.G. (2011) *Ichnology: Organism–Substrate Interactions in Space and Time*. Cambridge University Press, Cambridge, 358 p.

Catuneanu, O. (2006) *Principles of Sequence Stratigraphy*. Elsevier, Amsterdam, 375 p.

Collinson, J.D., Mountney, N.P. (2019) *Sedimentary Structures*. Dunedin Academic Press, Edinburgh, 310 p.

Cornet, A. (1952) L'Atlas saharien sud-Oranais- XIXèmeCong. Géol. Intern., Alger, Monographies régionales. 1ère sér., 12, 51p. 9 fig., 1 pl.

Delfaud, J. (1974) La sédimentation deltaïque ancienne. Exemples Sahariens. Bull. Centre. Recherches, Pau, SNPA, 8, 1, pp.241-263.

Douihasni, M. (1976) Etude géologique la région d'Aïn Ouarka-Boussemghoun (Partie centrale des Monts des Ksour) - Analyse structurale -Tome I : Stratigraphie. Thèse 3ème cyc. Oran : Université d'Oran, 115p, p208, fig. 49.

Duke, W.L. (1985) Hummocky cross-stratification, tropical hurricanes and intense winter storms. Sedimentology, 32, 167–194.

Dunham, R.J. (1962) Classification of carbonate rocks according to depositional texture. *In: Ham, W.E. (ed.), Classification of Carbonate Rocks*, AAPG Memoir 1, pp. 108–121.

Ekdale, A.A., Bromley, R.G., Pemberton, S.G. (1984) *Ichnology: Trace Fossils in Sedimentology and Stratigraphy*. SEPM Short Course No. 15, 317 p.

Elmi, S. (1978) Polarité tectono-sédimentaire pendant l'effritement des marges septentrionales du bâti africain au cours du Mésozoïque (Maghreb). Ann. Soc. geol. Nord, Lille, 97, 1-4, pp. 315-323.

Emberger, J. (1960) Esquisse géologique de la partie orientale des Monts des Ouled Naïl (Atlas saharien, Algérie) Publications du Service de la Carte géologique de l'Algérie 27, 1–398.

Embry, A.F., Klovan, J.E. (1971) A Late Devonian reef tract on northeastern Banks Island, NWT. *Bulletin of Canadian Petroleum Geology*, 19(4), 730–781.

Fairbridge, R.W., Bourgeois, J. (1978) The Encyclopedia of Sedimentology. Encyclopedia of Earth Sciences Series, Volume VI. xvi + 901 pp.

Flügel, E. (2010) *Microfacies of Carbonate Rocks: Analysis, Interpretation and Application*. Springer, Berlin, 984 p.

Folk, R.L., Land, L.S. (1975) Mg/Ca ratio and salinity: two controls over crystallization of dolomite: Am. Assoc. Petrol. Geol. Bull., v. 59, p. 60-68

Fürsich, F. T. (1995) Shell concentration, Eclogae geol. Helv. 88/3: 643-655 (1995)

Fürsich, F. T., Oschmann, W. (1986) Storm shell beds of Nanogyra in the Upper Jurassic of France, Neues Jahrbuch für Geologie und Paläontologie – Abhandlungen 172(2):141-161

Fürsich, F.T., Oschmann, W. (1993) Shell beds as tools in basin analysis: the Jurassic of Kachchh, western India. *Journal of the Geological Society*, 150(1), 169–185.

Gregory, M. R., Ballance, P. F., Gibson, G. W., and Ayling, A. M. (1979) On how some rays (Elasmobranchia) excavate feeding depressions by jetting water: Jour. Sed. Petrology, v. 49, p. 1125-1130

Guillemot J., Estorges P. (1981) Notice de la carte de Brézina au 1/200000. Direction de la Géologie, Direction des Mines et de la Géologie, Ministère de l'Industrie Lourde, Algérie, 45 p.

Guiraud R. (1973) Evolution post-triasique de l'avant-pays de la chaîne alpine en Algérie, d'après l'étude du bassin du Hodna et des régions voisines. Thèse de Doctorat ès-Sciences, Université de Nice : 270 p.

Herkat, M. (1982) Lithostratigraphie et sédimentologie des formations carbonatées du jurassique supérieur des monts des Oulad Nail et de la terminaison orientale du Djebel Amour (Atlas saharien). Thèse 3eme cycle, U-niv. Pau. 387p.

Kacemi, A. (2005) Cartographie et dynamique sédimentaire des séries du Dogger supérieur–Crétacé inférieur (Djara–Rhoundjaïa) des Monts des Ksour (Atlas saharien, Algérie). Mémoire de Magister, Université d'Oran, 212 p., 49 fig., 15 pl.

Kacemi, A. (2013) Évolution lithostructurale des Monts des Ksour (Atlas saharien, Algérie) au cours du Trias et du Jurassique : géodynamique, typologie des bassins et télédétection. Thèse de Doctorat, Université A.B.B. de Tlemcen, 229 p., p. 32, 6 fig.

Kazi-Tani. (1986) Evolution géodynamique de la bordure nord-africaine : le domaine intraplaque nord-algérien. Approche mégaséquentielle. Thèse Doctorat d'Etat, Pau, 2 tomes, 784 p., 361 fig.

Kidwell, S. M., Flessa, K. W., Brenchley, P. J. (1986) Conceptual Framework for the Analysis and Classification of Fossil Concentrations, Palaios 1(3):228

Kidwell, S.M., Holland, S.M. (1991) Field Description of Coarse Bioclastic Fabrics. SEPM Society for Sedimentary Geology

Lee, D.E., Williams, A., Brunton, C.H.C. (2006) *Treatise on Invertebrate Paleontology, Part H, Brachiopoda Revised*. Geological Society of America and University of Kansas.

Leonard, J.E., Cameron, B., Pilkey, O.H., Friedman, G.M. (1981) Evaluation of cold-water carbonates as a possible paleoclimatic indicator. *Sedimentary Geology*, 28(1), 1–28.

MacEachern, J.A and Bann, K.L. (2008) The role of ichnology in refining shallow marine facies models, in Hampson, G.J., Steel, R.J., Burgess, P. M and Dalrymple, R.W., eds., Recent Advances in Models of Siliciclastic Shallow-Marine Stratigraphy. SEPM Special Publication No 90, pp. 73-116.

Mahboubi M. (1983) Etude géologique du crétace post Aptient et du Tertiaire Continental de la bordure méridionale du Djebel Amour (Atlas Saharien Central). Tèse 3em cycle, IST, Univ. d'Oran. 161p.

Mahboubi, C.Y (2021) Les indices de fluides et diagenèse précoce dans les terrains du Jurassique de la région d'Aïn-Ouarka et d'El-Bayadh (Atlas Saharien, Algérie) Thèse Doctorat d'Etat, Univ. Oran, p67

MAHBOUBI, C.Y., RADULOVIĆ, B.V., OUALI MEHADJI, A., AYOUB-HANNAA, W., & MUNNECKE, A (2021a) Late Jurassic (Oxfordian–Kimmeridgian) brachiopods of the El-Bayadh Area (Central Saharan Atlas, Algeria): biostratigraphy, stratigraphic revision, Paleobiogeography and paleoecology. Historical Biology 121. https://doi.org/10.1080/08912963.2020.1861609 140

MAHBOUBI, C.Y., OUALI MEHADJI, A., & CHEVALIER, N (2021b) Microfacies and stable isotope features of the LOWER–MIDDLE Jurassic carbonate rocks of Western Saharan Atlas (Aïn Ouarka area, Algeria). Geological Journal gj.4149. https://doi.org/10.1002/gj.4149

Mahboubi, M., Bessedik, M., Belkebir, L., Adaci, M., Hebib, H., Bensalah, M., Mammeri, C., Mansour, B., Mansouri, M.-E.-H. (2007) Première découverte d'empreintes de pas de dinosaures dans le Crétacé inférieur de la région d'El Bayadh (Algérie). Bulletin du Service géologique de l'Algérie 18 (2): 127-139.

Mattauer, M., Tapponnier, P., Proust, F (1977) Les mécanismes de formation des chaînes intracontinentales : l'exemple des chaînes atlasiques du Maroc. Bulletin de la Société Géologique de France, S7–19, pp. 521–526.

Meddah, A., Bertrand, H., Elmi, S (2007) La province magmatique de l'Atlantique central dans le bassin des Ksour (Atlas saharien, Algérie), C. R. Géoscience 339 24–30, Science direct Elsevier.

Mekahli L., Elmi S., Benhamou M. (2004) Biostratigraphy, sedimentology and tectono-eustatic events of the Lower and Middle Jurassic of the Ksour Mountains. In : L. Guerrieri, I. Rischia, L. Serva, R. Pompili and E. Brustia (Eds.), Mem. Desc. della Carta Geologica d'Italia, 63 (5), pp. 37-54.

Mekahli, L. (1995) Hettangien au Bajocien supérieur des Monts des Ksour : Biostratigraphie, évolution paléogéographique et stratigraphie séquentielle. These de Doctorat d'État, Universite d'Oran, 358 p., 67 fig., 49 pl.

Miall, A.D. (1996) *The Geology of Fluvial Deposits. Sedimentary Facies, Basin Analysis, and Petroleum Geology. xvi + 582 pp*

Morizet M. (1970) – Contribution a l'étude géologique de la carte 1/200.000 de Brézina (Algérie) : secteur Nord – Nord-est. Mémoire de D. E. A., Université de Paris : 84 p.

Muniz, F., Bosence, D.W.J. (2018) Lacustrine carbonate platforms: Facies, cycles, and tectonosedimentary models for the presalt Lagoa Feia Group (Lower Cretaceous), Campos Basin, Brazil. AAPG Bulletin (2018)

Myrow, P.M., Southard, J.B. (1996) Tempestite deposition. Journal of Sedimentary Research (1996) 66 (5): 875–887.

Naimi M. N., Mahboubi C. Y., Cherif A. (2021b) Lithostratigraphy and evolution of the Lower Cretaceous Basins, in Western Saharan Atlas, Algeria: A comment. Journal of African Earth Sciences, 183 : 104304.

Naimi, M. (2022) Analyse ichnologique et reconstitution paléoenvironnementale de la série Albien–Turonien des Monts des Ouled Naïl. Thèse de 3eme cycle. Universite Kasdi Merbah – Ouargla, 193p

Nouar, O.B. (1992) Télédétection dans l'Atlas Saharien Central. Structures de réactivation dans le Djebel Amour d'après l'analyse d'images Landsat et SPOT. Mémoire de Magister, CNTS, Arzew, 106 p.

Ouali Mehadji, A. (1994) Brachiopodes des Monts des Ksour (Bajocien supérieur, Bathonien inférieur) (Atlas Saharien occidental, Algérie). Mémoire de Magister, Université d'Oran, 220 p.

Regagba, A. (2006) Étude sédimentologique et stratigraphique de la série du Jurassique moyen et supérieur de la région d'El Bayadh (Atlas Saharien central, Algérie). Mémoire de Magister, Université d'Oran, Algérie.

Reineck, H.E., Singh, I.B. (1980) *Depositional Sedimentary Environments*. Springer, Berlin, 551 p.

Remírez, I., Luis A. Spalletti; Manuel F. Isla; Ernesto Schwarz. (2022) Fine-grained distal deposits of a mixed siliciclastic–carbonate marine system: Origin of mud and implications on mixing processes, Journal of Sedimentary Research (2022) 92 (3): 210–231.

Ritter, E. (1902) Le Djebel Amour et les Monts des Ouled Naïl. Mémoires et Bulletins du Service de la Carte Géologique de l'Algérie, 2ème série : Stratigraphie, in-8°, 102 p., 16 fig., 4 pl.

Rodrigues, M.G., Varejão, F.G., Fürsich, F.T., Christofoletti, B., Matosí, S.A., Warren, L.V., Inglez, L., Cerri, R.I., Assine, M.L., Simões, M.G. (2024) Not all shell beds are made equal: Recognizing singular event-concentrations in megalakes. *Sedimentology*, 2024, 1–44.

Rodrigues, M.G., Varejão, F.G., Matos, S.A., Fürsich, F.T., Warren, L.V., Assine, M.L., Simões, M.G. (2022) High-resolution taphonomy and sequence stratigraphy of internally complex, bakevelliid-dominated coquinas from the Aptian Romualdo Formation, Araripe Basin, NE Brazil. *Marine and Petroleum Geology*, 143, 105814.

Sadji, R., et al. (2025) – "Pre-published"

Scholle, P.A., Ulmer, D.S. (2003) *A Color Guide to the Petrography of Carbonate Rocks: Grains, Textures, Porosity, Diagenesis*. AAPG Memoir 77.

Schreiber, B.C., Tabakh, M.E. (2000) Deposition and Early Alteration of Evaporates. Sedimentary Geology, 47, 215-238.

Strohmenger, C.J., Wirsing, G. (1991) A proposed extension of Folk's textural classification of carbonate rocks. Carbonat. Evaporit., 6: 23-28. 66

Tucker, M.E. (1991) *Sedimentary Petrology*. Blackwell Science, Oxford, 260 p.

Tucker, M.E., Wright, V.P. (1990) *Carbonate Sedimentology*. Blackwell Science, Oxford, 482 p.

Van Straaten, L.M.J.U. (1952) Biogenic textures and the formation of shell beds in the Dutch Wadden Sea.I. Koninkl. Nederl. Akad. Wettensch. Ser. 55, 500-516

Warren, J. (2000) Dolomite: Occurrence, Evolution and Economically Important Associations. Earth-Science Reviews, 52, 1-81.

Warren, J.K., Kendall, C.G.St.C. (1985) Comparison of Marine (Sub Aerial) and Salina (Subaqueous) Evaporates: Modern and Ancient. American Association of Petroleum Geologists Bulletin, 69, 1013-1023.Warren, J.K. (2000) – *Evaporites: Their Evolution and Economics*. Blackwell Science, Oxford, 480 p.

Williams, A., Carlson, S.J., Brunton, C.H.C., Holmer, L.E., and Popov, L., (1996) A supra-ordinal classification of the Brachiopoda: Philosophical Transactions of the Royal Society London, B. v. 351, p. 1171–1193.

Wright, V.P. (1992) A Revised Classification of Limestone. Journal of Sedimentary Geology, 76, 177-185.

Zhang, X., Pang, X., Jin, Z., Hu, T., Toyin, A., Wang, K. (2020) Depositional model for mixed carbonate-clastic sediments in the Middle Cambrian Lower Zhangxia Formation, Xiaweidian, North China. Advances in Geo-Energy Research, 4(1), 29–42.

List of Figures

Fig.1: Paleogeographic map of the Tethys during the Oxfordian 158.4 ma……..3

Fig.2: Geographic location and boundary of the Saharan Atlas with his three sections……3

Fig.3: Satellite picture showing the exact location of Dj Er Rokene next to the Sfissifa village…4

Fig.4: Log synthetizing the late Jurassic formation of El Bayadh region……11

Fig.5: Map of the north African showing the main structural features of the atlas 1.Transversal of the Moulouya ; 2.Transversal of the Tafna-Magoura ; 3.Transversal of the Ain Séfra – Saida ; 4.Transversal of the El-Bayadh- Tiaret ; 5.Transversal of the Theniet El Had ; 6.Transversal of the Aurès – Hodna……12

Fig.6: Google earth image showing the localization of the Sfissifa outcrop section , the red star marks the beginning of the section…..……18

Fig.7: Lithostratigraphic log of the Sfissifa Formation El Bayadh. (A) Shoal limestones and the first carbonates beds of the formation. (B) Disarticulated oyster shells. (C) Brachiopods fossils in silty marls and the first brachiopods level. (D) Sandstone-marl alternation and the first terrigenous deposits of the formation……20

Fig.8: Massive package of limestones with shell beds intercalation ; (B) Alternating white and dark gypsum beds ; (C) Complete oysters shells ; (D) Erosive base below limestone bed ; (E) Trough-cross beddings sedimentary structure ; (F) Parallel laminations ; (G) First brachiopods level with a close up look ; (H) Mark lest by a gastropod shell……23

Fig.9: Panoramic photograph showing the Sfissifa Formation and the Continental Intercalaire; (B) Alternating sandstone layers with green marls ; (C) Second brachiopod level ; (D) Bioturbated oolitic limestone ; (E) HCS ; (F) Languid ripples ; (G) Massive dolostone beds……...…24

Fig.10: Upper Kimmeridgian *Xestosina arguta* (transition from the Eudoxus Zone to base of the Autissiodorensis Zone), Djebel e Roken, El Bayadh area, Sfissifa Formation . dorsal B, ventral C, lateral D, and front A views. (scale 3cm). (member 01, 50m)…….25

Fig.11: early Tithonian *Xestosina sera* representing the *Gigas* Zone (*Gravesiana* Subzone), Djebel e Roken, El Bayadh area, Sfissifa Formation . dorsal B, ventral C, lateral D, and front A views. (scale 3cm). (member 02, 81m)…….…….26

Fig.12: Upper Jurassic oysters: ?Africogryphaea geniculata n. sp (member 02, 53m). B: Pseudexogyra euryhalina n. gen. and n. sp (membre 3), dorsal 2, ventral 1. (scale 3cm). (and Djebel e Roken, El Bayadh area, Sfissifa Formation) …….…….…….27

Fig.13: (A) and (H): Shell beds , member 02 ; (C): Oolitic limestone, member 2 ; (D): Dolostone bed, member 03 ; (E) gypsum layers alterning with marls, member 01……32

Fig.14: (A) and (H): Hummocky cross stratifications in sandstones showing erosive base (red line in fig H) and with highlighted laminas, member 03, 86m ; (B): Erosive base in the dolostones, member 3, 97m ; (C): Languid ripples on top of the HCS sandstones, member 03, 86m ; (D): Trough cross-beddings from the second shell bed of the formation, member 02, 56m ; (E): Trough cross-beddings on dolostones, member 03, 99m ; (F): Parallel laminations, member 02, 62m ; (G): Close up look on the horizontal burrows from the intense bioturbation on the oolitic limestones of the second member, member 03, 88m……33

Fig.15: columnar section of sfissifa Formation organized into three member displaying microfacies data (Sf1-Sf20 sample taken)…….40

Fig.16: A: Microphotographs of the main characteristic microfacies of the Sfissifa Formation. A: (member 02,sample Sf 1, 50m) Rudstone composed of closely packed bivalve shells (> 2 mm), accompanied by concentric ooids exhibiting partial to complete micritization, all set within a micritic matrix; B: a closer look at A; C: (member 02,sample Sf 1, 50m) Floatstone displaying scattered bivalve shells >2mm in a micritic dominated matrix; D:(member 02, sample Sf 3, 56m) Floatstone composed of bivalve shells scattered in a micritic matrix; E:(member02,sample Sf 4, 59m) Show a rudstone composed of bivalves, with abundant quartz grains and a few echinoderm fragments embedded in a micrite matrix; F:(member 02, sample Sf 6, 62m) same texture as D however with a lesser abundance of quartz grains; G:(member 02, sample Sf 8, 68m) same texture……42

Fig.17: Microphotographs of the main characteristic microfacies of the Sfissifa Formation H:(member 02, sample Sf 10, 70m) Packstone primarily composed of micritized concentric ooids,

associated with bioclasts smaller than 2 mm, all enveloped in a micritic matrix ; I:(member 02, sample Sf 11, 71m) Grainstone composed of the same components as E, but with a matrix dominated by sparite ; J:(member 03, sample Sf 16, 89m) Packstone made only of micritized ooids closely packed in a micrite dominated matrix ; K:(member 03, sample Sf 17, 90m) Floastone containing gastropods >2mm scattered along side bivalve fragments in micrite ; L:(member 03, sample Sf 19, 91m) Rudstone composed of closely packed fragmented bivalves within a micritic matrix ; M:(member 03, sample Sf 20, 96m) Dolostone unclear structure that show probable dolomitized shells……...43

Fig.18: The key factors controlling shell concentration formation (Franz., 1995)……..51

Fig.19: the descriptive classification of shells concentrations (Franz., 1995)…….54

Fig.20: (A): Centimetric disarticulated oysters shells ; (B): Thin shell bed with visible oysters shell fragments ; (C)\(D): Beds of shell beds and oolitc limestone ; (E): Plain view of a shell concentration made from oysters shells ; (F): close up look at E…….56

List of Tables

Table 1: comparison between the old and new subdivision of the upper Jurassic of El Bayadh……...15

Table 2: A Classification of carbonates rocks (Dunham 1962); **B** : Classification of (Embry and Klovan 1972)……..38

Table 3: Full and summarized inventory of the facies and sedimentary structures with their interpretations……....48

Table 4: Full and summarized inventory of the microfacies data and their energetic interpretations……..……..49

Table 5: samples taken exact locations in the Sfissifa form……...…….50